

Vehicle Routing Problems in the Age of Semi-Autonomous Driving

Hins Hu¹ and Samitha Samaranyake²

¹Systems Engineering, Cornell University, zh223@cornell.edu

²School of Civil and Environmental Engineering, Cornell University, samitha@cornell.edu

Abstract

We are in the midst of a semi-autonomous era in urban transportation in which varying forms of vehicle autonomy are gradually being introduced. This phase of partial autonomy is anticipated by some to span a few decades due to various challenges, including budgetary constraints to upgrade the infrastructure and technological obstacles in the deployment of fully autonomous vehicles (AV) at scale. In this study, we introduce the *vehicle routing problem in a semi-autonomous environment* (VRP-SA) where the road network is not fully AV-enabled in the sense that a portion of it is either not suitable for AVs or requires additional resources in real-time (e.g., remote control) for AVs to pass through. Moreover, such resources are scarce and usually subject to a budget constraint. An exact mixed-integer linear program (MILP) is formulated to minimize the total routing cost of service in this environment. We propose a two-phase algorithm based on a family of *feasibility recovering sub-problems* (FRP) to solve the VRP-SA efficiently. Our algorithm is implemented and tested on a new set of instances that are tailored for the VRP-SA by adding stratified grid road networks to the benchmark instances. The result demonstrates a reduction of up to 37.5% in vehicle routing costs if the fleet actively exploits the AV-enabled roads in the environment. Additional analysis reveals that cost reduction is higher with more budget and longer operational hours.

1 Introduction

With the development of numerous advanced technologies related to autonomous driving, such as smart sensors, computer vision, and high-speed wireless communication, the deployment of autonomous vehicles (AV) fleets in all kinds of transportation is becoming more and more viable. More importantly, replacing human-driven vehicles (HDV) with AVs in many businesses may potentially reduce the operational cost dramatically as drivers' wages contribute a great portion of it. In the trucking industry, according to a report [28] by the American Transportation Research Institute, the driver-based cost contributed 35.8% of the average marginal cost per mile in 2011 and this number climbed up to 40.2% in 2022 due to increases in labor costs. If we deduct the amortized cost of vehicle purchases and leases, the percentage of the driver-based cost to the operational cost per mile in 2011 and 2019 are 37.6% and 47.2% respectively.

Although the AV industry has seen significant advancements and substantial investment, a fully autonomous driving environment remains years away. The era of *semi-autonomous driving* is expected to persist for several decades due to numerous barriers. First, key technologies such as motion planning and object detection continue to pose significant bottlenecks. According to SAE International’s classification system [23], autonomous driving is categorized into six levels, ranging from level 0 (no automation) to level 5 (full automation). As of March 2021, Honda became the first manufacturer to offer a legally approved level-3 vehicle [4], capable of autonomous driving in certain conditions, though human intervention is still required in some situations. Second, mixed traffic environments, with both AVs and HDVs, are inevitable due to factors such as consumer preference and the long service life of traditional automobiles. A survey on commuting preferences [19] conducted with 721 participants found that many individuals remain hesitant to adopt AVs. Even with a fully subsidized shared AV service, 44% of respondents still preferred regular vehicles, and only 75% expressed interest in switching to shared AVs. Third, achieving full automation in some scenarios is more challenging than in others. For example, high-density urban areas, compared to long-haul truck platooning, present greater complexity for level-5 automation due to intricate road networks, frequent interactions between vehicles and pedestrians, and the existence of traffic control. Fourth, autonomous driving requires significant infrastructure upgrades, particularly in vehicle-to-infrastructure (V2I) communication systems, to facilitate precise AV maneuvers such as lane-changing and merging. However, the investment required for these upgrades is often constrained by budgetary limitations, making it a long-term undertaking. Finally, legislative and policy frameworks tend to lag behind technological development. Concerns around safety, equity, and privacy often drive a more conservative approach to regulating autonomous driving, further delaying widespread adoption.

Given the limitations aforementioned, new challenges arise when deploying AVs in a semi-autonomous environment. Specifically, road networks are not fully accessible to AV fleets in the sense that certain levels of AVs may be prohibited from traversing a subset of road segments, leading to a classification of roads based on their compatibility with different levels of AV autonomy. In the simplest case, the road network can be modeled as a bi-level system comprising *ordinary roads* and *AV-enabled roads*. Additionally, a critical feature of the semi-autonomous environment is that not all AVs operate at full autonomy (i.e., level 5). Some may require external resources, such as real-time remote control, to navigate AV-enabled roads. These resources, however, are typically costly. For instance, in October 2020, Waymo launched a geo-fenced semi-autonomous ride-hailing service in Phoenix, U.S., supported by a team of remote engineers available to intervene in contingencies [20]. Similarly, Enride has deployed electric autonomous trucks on low-traffic private roads within logistics and manufacturing hubs and is working toward operating them on public roads with remote supervision [16].

With that said, optimal vehicle dispatching and routing strategies at the operational level, traditionally modeled by the vehicle routing problem (VRP), need to be re-examination and re-designed, particularly for high-density urban areas. Moreover, vehicle dispatching schedules are

crucial because the simultaneous demand for resources by all AVs must not exceed the maximum capacity. Exceeding this capacity can result in system failures with severe consequences, such as collisions. From a resource allocation perspective, fleet operators need to assign resources to AVs effectively by designing vehicle schedules based on prior knowledge of road networks. To address these new challenges, a holistic optimization approach is essential. Therefore, we propose a novel variant of the VRP, termed the *Vehicle Routing Problem in the Semi-Autonomous Environment* (VRP-SA).

The contribution of our work is threefold: (1) We formalize a novel vehicle routing problem called VRP-SA to address the new challenges of deploying AV fleets in a semi-autonomous environment. (2) We provide a practically efficient solution approach for the VRP-SA. (3) We analyze the impact of varying unit routing costs and the density of AV-enabled roads on the deployment of AVs in the age of semi-autonomous driving.

The paper is organized as follows: Section 2 briefly reviews the history of VRP and relevant literature on VRP variants involving mixed fleets and limited resources. Section 3 presents a formal description of the VRP-SA. Section 4 introduces an exact mixed-integer linear program (MILP) for the VRP-SA. Section 5 discusses some extended studies in the MILP to enhance the model’s comprehensiveness and adaptability. Section 6 presents a two-phase algorithm based on a family of feasibility recovering sub-problems (FRP) to solve the VRP-SA efficiently. Section 7 presents a new set of instances tailored for the VRP-SA and analyzes the results of numerical experiments conducted on these instances. Section 8 concludes the paper and outlines potential directions for future research.

2 Literature Review

VRP was first formulated as an integer linear program by Dantzig and Ramser [10] in 1959. The seminal heuristic algorithm to solve it was developed by Clark and Wright [9] in 1964. The proof of the NP-hardness of VRP was provided by Lenstra and Kan [27] in 1981. In addition to these milestones, extensive studies in VRP models (e.g. [18] [25] [40] [38] [12] [41]), construction heuristics (e.g. [17] [14] [6]), meta-heuristics (e.g. [21] [3] [36]), branch-and-bounds approaches (i.e., [11] [13] [15]), and learning-based approaches (e.g. [35] [26] [29]) have been conducted and published over the past decades. Numerous benchmark data sets (e.g. [42] [1] [44]) have also been created to support the performance tests of newly-developed VRP algorithms. The most recent research on VRP follows a trend toward designing a general-purpose algorithm by the hybridization of various frameworks to solve a wide range of VRP variants efficiently and on a larger scale. The representative work is the unified hybrid genetic search (UHGS) developed by Vidal et al. [46]. More comprehensive literature reviews from different aspects of VRP are referred to these papers ([7] [8] [34] [24] [31] [5]) and this book [43].

A key feature of the VRP-SA is its mixed fleet of AVs and HDVs, which can be modeled by the family of Heterogeneous Fleet Vehicle Routing Problems (HFVRP) involving only two types

of vehicles. This topic is covered in a chapter by Toth and Vigo [43]. The HFVRP family can be further refined into different categories depending on fleet constraints (limited or unlimited) and cost structures (vehicle-dependent or vehicle-independent). Research on exact approaches for the HFVRP is relatively limited. The most effective exact approach currently available is the branch-and-cut-and-price algorithm developed by Baldacci and Mingozzi [2]. In contrast, most existing approaches are heuristic-based, such as the multi-start adaptive memory programming (MAMP) by Li et al. [30], the variable neighborhood search (VNS) by Imran et al. [22], and the memetic algorithms by Prins [37]. Currently, the UHGS approach [46] is recognized as the leading method for the HFVRP.

One recent work by Molina et al. [33] also discussed the VRP with a limited number of resources available. However, their focus is on scenarios where resource limitations—such as drivers, vehicles, or other equipment—prevent the servicing of all customers. This contrasts with our work, where limited resources (e.g., remote control) shared across the entire AV fleet can influence the routing decisions of individual vehicles when serving multiple customers.

3 The Problem Statement of VRP-SA

The VRP-SA admits the following inputs: (1) A directed graph $G = (V, E = E^a \cup E^o)$ representing the underlying road network, where V is the set of nodes representing road intersections, and E^a and E^o are the sets of edges representing AV-enabled and ordinary road segments, respectively. (2) A depot $o \in V$ from which all vehicles depart and to which they return after the service. (3) A time horizon $[0, T]$ of operations (e.g., a day). (4) A set of customers $D \subset V$ with a demand vector $\mathbf{d} \in \mathbb{R}_{++}^{|D|}$. (5) A mixed vehicle fleet $M = M^a \cup M^h$, where M^a is the set of AVs and M^h is the set of HDVs, all with identical capacity $W \in \mathbb{R}_{++}$. (6) A pair of fixed costs (f^a, f^h) of dispatching an AV and an HDV, respectively. (7) A vector of routing costs $\mathbf{c} \in \mathbb{R}_{++}^{3 \times |E|}$, where each cost is associated with a road segment in E and varies by vehicle type and road type. The cost structure is detailed in Table 1. Here, c_e^1 and c_e^2 represent the routing costs for an AV traveling on an AV-enabled road segment $e \in E^a$ and an ordinary road segment $e \in E^o$, respectively. Similarly, c_e^0 denotes the routing cost for an HDV traversing any road $e \in E$, regardless of type. Two constant cost adjustment factors, η_1 and η_2 , are applied uniformly across all edges. (8) A vector of travel times $\Delta \mathbf{t} \in \mathbb{R}_{++}^{|E|}$, with each entry corresponding to a road segment. (9) A budget $B \in \mathbb{N}_+$ representing the number of remote controllers available to assist AVs in real-time while they are traversing ordinary road segments. All aforementioned notations are summarized in Table 2 for reference in later sections.

	AV-Enabled Roads	Ordinary Roads
AVs	$c_e^1 = \eta_1 \cdot c_e^0$	$c_e^2 = \eta_2 \cdot c_e^0$
HDVs	c_e^0	c_e^0

Table 1: The routing cost structure of a vehicle traversing road segment e

The problem is subject to the following assumptions: (1) HDVs can traverse the entire road network freely without external resources, whereas AVs require additional support from remote controllers to pass through ordinary roads. Specifically, an AV locks one remote controller upon entering an ordinary road from an AV-enabled road and releases it upon returning to an AV-enabled road. (2) As outlined in Table 1, the routing cost for a vehicle on a given road segment depends on both the vehicle and road types. We further assume that, in the age of semi-autonomous driving, the routing cost for an AV on an AV-enabled road is lower than that for an HDV on the same road (i.e., $\eta_1 < 1$). Conversely, on an ordinary road, the cost for an AV exceeds that of an HDV (i.e., $\eta_2 > 1$). This assumption is justified by the significant cost reduction from eliminating driver-related expenses on AV-enabled roads. However, on ordinary roads, the scarcity and high cost of remote controllers lead to increased operational expenses, surpassing even the driver-related portion. (3) The dispatched times for vehicles are flexible within $[0, T]$, provided that all vehicles return to the depot before T .

The objective of the VRP-SA is to find a minimum-cost dispatching and routing strategy that serves all customers while satisfying the budget constraint of remote controllers, the return time constraints, and the capacity constraints. The fixed costs for establishing the real-time remote control system are treated as overheads and thus excluded from our decision making. Additionally, we do not integrate other commonly seen conventional constraints, such as time windows for customers and the order of pick-up and delivery, as they are relatively independent of the core issues addressed in this paper.

4 The Mixed-Integer Linear Program

In this section, we will first briefly discuss a challenge of formulating the VRP-SA as a mixed-integer linear program (MILP). Next, we will establish a connection between a key characteristic of the VRP-SA and a simpler classical combinatorial optimization problem known as the *Steiner Traveling Salesman Problem* (STSP). Leveraging several properties of the STSP, we will then demonstrate how to construct an *expanded graph* based on the original road network and derive an exact MILP formulation for our problem on this expanded graph.

Many VRP models and algorithms are formulated and designed based on the *metric closure* of the underlying road network [43]. The metric closure of a graph G on a subset of nodes D is a complete graph \overline{G} on D , where each edge is weighted by the cost of the shortest path between the two corresponding nodes in G . This transformation allows each vehicle route in the solution to be represented as an ordered sequence, indicating the order of serving the subset of customers assigned to that vehicle. The low-level routing in the real-world road network is pre-determined by computing the minimum-cost paths between all pairs of customers. This trick significantly reduces the number of decision variables and constraints required to model a VRP, resulting in a more compact formulation. For instance, it ensures that each customer node is visited exactly once in the optimal solution, enabling the use of a constraint akin to unit flow conservation [10]. This

pre-processing step, which transforms the underlying network into its metric closure, is illustrated in Figure 1.

However, this trick is not applicable to the VRP-SA due to the presence of mixed road types in the underlying network. While shortest paths can still be pre-determined, a vehicle may not always travel along the shortest path between two customers in the optimal solution. This is because its ability to navigate an ordinary road segment depends on the continuous availability of a remote controller during the entire period it remains on the segment, from entry to exit. Consequently, the feasibility of selecting ordinary road segments for different AV routes is interdependent and constrained by a real-time enforced budget. Figure 1 further demonstrates that, once the network is transformed into its metric closure, all information about the road type of each edge is lost.

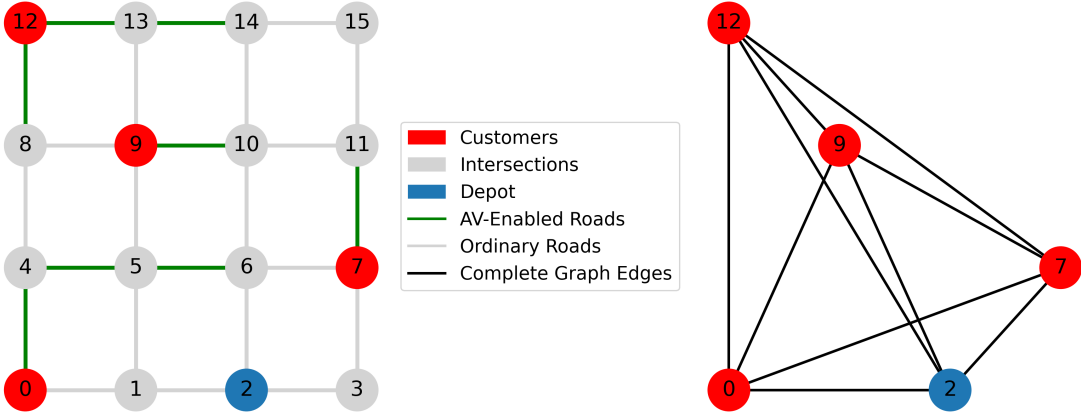


Figure 1: A toy example of a road network of mixed road types and its metric closure

Therefore, to formulate an MILP for the VRP-SA, we must work directly on the original road network. A key characteristic of an optimal solution to the VRP-SA in the original network is that any node may be visited more than once if necessary, which features the STSP in its most basic form. The formal definition of the STSP is as follows: Given an undirected and connected graph, a subset of nodes designated as required nodes to be served, a distinguished required node serving as the depot, and positive costs associated with all edges, the objective is to determine a minimum-cost route that visits all required nodes. Essentially, the Steiner version of the TSP relaxes the requirement for the graph to be complete [39]. We identify the following two lemmas of the STSP, with formal proofs provided in Appendix A.

Lemma 4.1. *In an optimal solution to the STSP in a directed graph, a node can be visited at most n times, where n is the number of required nodes in the graph.*

Lemma 4.2. *In an optimal solution to the STSP in a directed graph, an edge can be traversed at most $n - 1$ times, where n is the number of required nodes in the graph.*

The observations in Lemma 4.1 and Lemma 4.2 can be naturally extended to the VRP-SA. Specifically, for each node in the set V , an upper bound on the number of times it can appear in

an optimal solution to the VRP-SA can be established. This result is presented in Proposition 4.3, with a detailed proof provided in Appendix A.

Proposition 4.3. *Let $P(m)$ be the route of vehicle m in the optimal solution to the VRP-SA. Let W be the capacity of vehicle m . Let $\{d_i : i = 1, \dots, |D|\}$ be a non-decreasing sequence indicating the demands of customer set D . Then, a node $v \in P(m)$ can be visited by vehicle m at most $k + 1$ times, and an edge (u, v) , $\forall u, v \in P(m)$ can be traversed by vehicle m at most k times, where k is defined as the largest integer $j = 1, \dots, |D|$ satisfying $\sum_{i=1}^j d_i \leq W$.*

Building on the result of Proposition 4.3, we propose an approach to formulate an exact MILP for the VRP-SA by constructing a k -layer expanded graph G_e from the original network graph G , where k is the number defined in Proposition 4.3. The construction process is as follows:

1. Duplicate G by k times and stack them in layers.
2. Create an dummy node s called the *sink depot* on the base layer.
3. For every two adjacent layers, add an dummy directed edge pointing from every customer on the lower layer to its duplicate customer on the upper layer.
4. For every duplicate depot on the duplicate layers, add an dummy directed edge pointing from the depot to the sink depot s .
5. Assign zero cost and zero travel time to each dummy edge.

Accordingly, additional notations are introduced to account for duplication in the expanded graph and to support the MILP formulation later in this section. These notations are clearly explained and summarized in Table 2, so their definitions will only be repeated in the text when necessary.

Figure 2a visualizes an example of a 3-layer expanded graph of a small undirected road network. Two upper layers in dashed lines are duplicated from the base layer in solid lines. The dots in sky blue are depots in O . The dots in light purple are customers in D_e . The black dots are road intersections in $V_e \setminus (O \cup D_e)$. The bold dashed arrows are dummy edges in A .

The necessity of constructing the k -layer expanded graph arises from two key considerations: (1) each node or edge in the network, except the depot, can be visited up to k times by a vehicle, and (2) we have to track the timestamps whenever a vehicle transitions between ordinary roads and AV-enabled roads so that we can count the total number of occupied remote controllers at any given moment. The expanded graph provides an additional dimension to distinguish between different times a vehicle visits the same node or traverses the same edge. It is important to note that this expanded graph is not *strongly connected*, as nodes on lower layers are not reachable from nodes on upper layers. Thus, if we can introduce a properly designed constraint in the MILP that forces a vehicle to move up one layer via an dummy edge every time it serves a customer, each node in V_e is guaranteed to be visited by the vehicle at most once in the optimal solution to the VRP-SA.

Notation	Definition
G	The graph representing the underlying road network
V and E	The entire set of nodes and edges in graph G
E^a and E^o	The set of edges representing AV-enabled and ordinary roads
D	The set of customers
\mathbf{d}	The demand vector of customers
M	The entire set of vehicles
M^a and M^h	The set of AVs and HDVs
W	The uniform capacity of all vehicles
\mathbf{c}	The vector of edge-wise routing costs
f^a and f^h	The fixed costs of dispatching an AV and an HDV
η_1 and η_2	The cost adjustment factors for AVs on two types of roads
$\Delta \mathbf{t}$	The vector of edge-wise travel times
T	The end time of operation
G_e	The expanded graph
k	The number of layers in the expanded graph
o and s	The source and sink depot on the base layer of G_e
V_e and E_e	The set of nodes and edges in G_e
E_e^a and E_e^o	The set of AV-enabled and ordinary edges in E_e
D_e	The set of customers in G_e , including duplicates
O	The set of depots in G_e , including duplicates
$D^H(i)$	The set of duplicate customers on layer $i \in [k]$
$D^V(i)$	The set of customers duplicated from a single customer $i \in D$
A	The set of dummy edges connecting layers in G_e
$\delta^-(i)$ and $\delta^+(i)$	The set of outgoing and incoming neighbor nodes of $i \in V_e$
Q	The set of discretized time intervals in $[0, T]$
a_q and b_q	The start and end time of interval $q \in Q$
B	The budget of remote controllers
S	The Cartesian product of sets M^a and E_e^o

Table 2: Notations

Figure 2b visualizes this idea using the same expanded graph from Figure 2a. Assuming sufficient vehicle capacity, the optimal solution follows the minimum-cost paths to serve two customers and then returns via the same paths in reverse. The red path in the figure represents the optimal vehicle route in the expanded graph, ensuring that no node or edge is visited more than once.

Now, we are ready to formulate an MILP for the VRP-SA. We emphasize that it is based on the k -layer expanded graph G_e instead of the original road network G . To keep track of the timestamps in different vehicle routes, we adopt the three-index formulation [43]. Define a binary decision variable x_{ijm} for every $(i, j) \in E_e$ and every $m \in M$, with $x_{ijm} = 1$ indicating vehicle m traverses edge (i, j) in the expanded graph G_e . Let \mathbf{x} be the vector of all x_{ijm} . Define a binary decision variable y_{om} for every $m \in M$, with $y_{om} = 1$ indicating vehicle m is dispatched. Let \mathbf{y}_o be the vector of all y_{om} . The objective is to minimize the total operational cost, which includes both

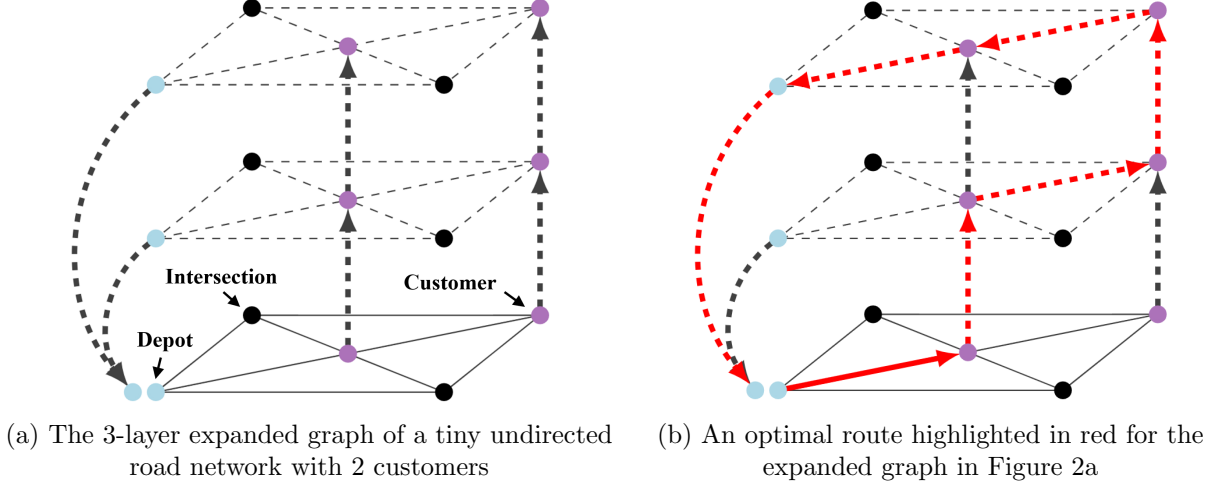


Figure 2: Visualization of a 3-layer expanded graph

the routing cost, $RC(\mathbf{x})$, and the fixed cost of vehicle dispatching, $FC(\mathbf{y}_o)$.

$$\min_{\mathbf{x}, \mathbf{y}_o} RC(\mathbf{x}) + FC(\mathbf{y}_o) \quad (1)$$

Specifically, the routing cost in Equation 2 consists of three terms to account for the cost structure described in Table 1. The fixed cost in Equation 3 depends on the number of dispatched vehicles of each type (i.e. AVs and HDVs).

$$RC(\mathbf{x}) = \sum_{(i,j) \in E, m \in M^h} c_{ij}^0 x_{ijm} + \sum_{(i,j) \in E_e^a, m \in M^a} c_{ij}^1 x_{ijm} + \sum_{(i,j) \in E_e^o, m \in M^a} c_{ij}^2 x_{ijm}, \quad (2)$$

$$FC(\mathbf{y}_o) = f^a \sum_{m \in M^a} y_{om} + f^h \sum_{m \in M^h} y_{om}. \quad (3)$$

Constraints 4 and 5 reflect the law of flow conservation for vehicle dispatching. Constraint 4 states that, for each vehicle and each node except the source depot o and the sink depot s , the amount of incoming flow must be equal to the amount of outgoing flow. Constraint 5 states that every vehicle, if dispatched from the source, must enter the sink ultimately. The flow value is capped by one unit to ensure that a vehicle does not return to the same node or edge in the expanded graph.

$$\sum_{j \in \delta^-(i)} x_{ijm} = \sum_{j \in \delta^+(i)} x_{jim}, \quad \forall i \in V_e - \{o, s\}, \forall m \in M, \quad (4)$$

$$\sum_{j \in \delta^-(o)} x_{ojm} = \sum_{j \in \delta^+(s)} x_{j sm} \leq 1, \quad \forall m \in M. \quad (5)$$

Define a binary decision variable y_{im} for every $i \in D_e$ and every $m \in M$, with $y_{im} = 1$ indicating

vehicle m serves a duplicate of customer i in the expanded graph. Together with the previously defined decision variables \mathbf{y}_o , we interpret $y_{im} = 1$ for all $i \in D_e \cup \{o\}$ as an indicator of whether a vehicle serves a required node, either a customer or the depot.

Constraints 6 and 7 are typical in other VRP formulations but have been adapted in our MILP to ensure compatibility with the expanded graph. Constraint 6 states that each customer is served by exactly one vehicle in total, though it may be served on any layer in the expanded graph. Constraint 7 enforces that the total demand assigned to a vehicle does not exceed its capacity.

$$\sum_{i \in D^V(j)} \sum_{m \in M} y_{im} = 1, \quad \forall j \in D, \quad (6)$$

$$\sum_{i \in D_e} y_{im} d_i \leq W, \quad \forall m \in M. \quad (7)$$

Constraint 8 ensures that a vehicle can visit a customer node without necessarily serving it. This situation arises when this customer lies on a vital path for a vehicle to reach another customer. In another word, a pass-through visit is allowed (i.e., $y_{im} = 0$ but $\sum_{j \in \delta^+(i)} x_{jim} = 1$).

$$\sum_{j \in \delta^+(i)} x_{jim} \geq y_{im}, \quad \forall i \in D_e, \forall m \in M. \quad (8)$$

Constraint 9 is called the transition constraint that guarantees a vehicle has to move to the upper layer after serving one customer. If vehicle m does not serve a customer (i.e., $y_{im} = 0$), though it might have passed it, the vehicle stays on the same layer, which means $x_{ijm} = 0$ for dummy edge $(i, j) \in A$. Otherwise, the vehicle has to move up one layer, which means $x_{ijm} = 1$.

$$x_{ijm} = y_{im}, \quad \forall (i, j) \in A, \forall m \in M. \quad (9)$$

Then, we need a valid *sub-tour elimination constraint* (SEC) to prevent a feasible route from being disconnected to the depot. In the context of VRP-SA, it is natural to devise the SEC in the Miller-Tucker-Zemlin (MTZ) form [32] when continuous variables (e.g., the timestamps) are necessary for the formulation. We define a continuous decision variable $t_{im} \in [0, T]$ for every $i \in V_e$ and every $m \in M$ to represent the timestamp of vehicle m visiting node i . In particular, t_{om} represents the departure time of vehicle m in real-world operation.

Constraints 10 and 11 correspond to the SEC in the MTZ form. Constraint 10 states that the timestamp of a vehicle visiting a node should be strictly larger than any timestamps of the same vehicle visiting the predecessors. It prevents identical timestamps of different nodes in the same route, which eliminates sub-tours. The existence of Constraint 11 makes the inequalities in Constraint 10 become equalities if they are associated with a vehicle route (i.e., $x_{ijm} = 1$), which ensures that all timestamps in a route are consistent with respect to the travel time. Additionally,

the operational end time is set as an upper bound for t_{sm} to prevent any late return of vehicles.

$$t_{jm} \geq t_{im} + \Delta t_{ij} + T(x_{ijm} - 1), \quad \forall (i, j) \in E_e, m \in M, \quad (10)$$

$$T \geq t_{sm} = t_{om} + \sum_{(i,j) \in E_e} \Delta t_{ij} x_{ijm}, \quad \forall m \in M. \quad (11)$$

Up to this point, we are able to keep track of all timestamps by decision variables. The next step is to formulate the budget constraint. We discretize the time horizon $[0, T]$ into a set of disjoint but connecting intervals $[a_q, b_q]$, $\forall q \in Q$, where Q is the set of interval indices. Mathematically, $b_q = a_{q+1}$ holds for $q = 1, \dots, |Q| - 1$. In practice, the intervals are set to be short (e.g., one minute) and can be equal. Then, we restrict the total number of occupied remote controllers, which is equivalent to the total number of AVs on ordinary roads simultaneously, to be less than the budget during any time interval q .

For each $q \in Q$ and each $m \in M^a$, we define a binary decision variable u_{qm} , where $u_{qm} = 1$ indicates that vehicle m is in need of a remote controller during the q -th time interval. Note that we only consider AVs since HDVs are not subject to the budget constraint. Then, $u_{qm} = 1$ if vehicle m is traveling along edge $(i, j) \in E_e^o$ during $[t_{im}, t_{jm}]$ and $[a_q, b_q]$ overlaps with $[t_{im}, t_{jm}]$. The overlapping relation can be described by two conditions:

1. The timestamp when vehicle m enters edge (i, j) has to be earlier than the end of the q -th time interval.
2. The timestamp when vehicle m leaves edge (i, j) has to be later than the start of the q -th time interval.

Figure 3 illustrates such an overlapping relation. Suppose $[a_{10}, b_{10}]$ is the time interval of interest. $[t_1, t_2]$ and $[t_5, t_6]$ overlap with $[a_{10}, b_{10}]$ because both of the aforementioned conditions hold. $[t_8, t_9]$ does not overlap with $[a_{10}, b_{10}]$ because $t_8 > b_{10}$. More formally, $u_{qm} = 1$ if the following three

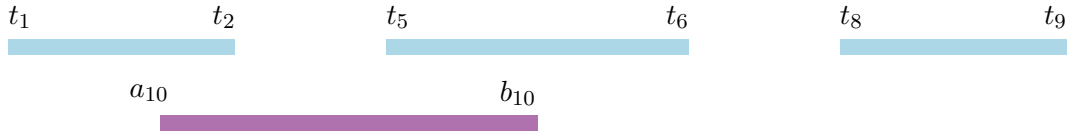


Figure 3: The relation of the overlapping relation between $[a_q, b_q]$ and $[t_{im}, t_{jm}]$

conditions hold: (1) $x_{ijm} = 1$, (2) $a_q \leq t_{jm}$, and (3) $t_{im} \leq b_q$. Define a binary decision variable α_{qijm} for every time interval $q \in Q$, every edge $(i, j) \in E_e^o$, and every AV $m \in M^a$ to indicate whether $a_q \leq t_{jm}$. We have $a_q \leq t_{jm}$ if and only if $\alpha_{qijm} = 1$. By analogy, we define β_{qijm} to indicate whether $t_{im} \leq b_q$.

To capture such sufficient and necessary conditions, we can formulate Constraints 12 to 15 for

every time interval $q \in Q$ and every vehicle-edge tuple $(m, (i, j)) \in S = M^a \times E_e^o$.

$$t_{jm} \leq a_q + T \alpha_{qijm}, \quad (12)$$

$$t_{jm} \geq a_q + T (\alpha_{qijm} - 1), \quad (13)$$

$$b_q \leq t_{im} + T \beta_{qijm}, \quad (14)$$

$$b_q \geq t_{im} + T (\beta_{qijm} - 1). \quad (15)$$

Next, Constraint 16 is formulated to describe the sufficient condition for $u_{qm} = 1$.

$$u_{qm} \geq \frac{1}{3}(\alpha_{qijm} + \beta_{qijm} + x_{ijm}) - \frac{2}{3}, \quad \forall q \in Q, \forall (m, (i, j)) \in S. \quad (16)$$

The last but not least, we count how many remote controllers are occupied by the AV fleet during every time interval and cap it by the budget, which leads to Constraint 17.

$$\sum_{m \in M^a} u_{qm} \leq B, \quad \forall q \in Q. \quad (17)$$

The MILP is of polynomial size with respect to the size of the expanded graph and the number of discrete time intervals. The total number of decision variables and the total number of constraints are both $\mathcal{O}(k |S| |Q|) = \mathcal{O}(k |E_e^o| |M^a| |Q|)$. To summarize, the complete MILP is shown as follows.

$$\begin{aligned}
& \min_{\mathbf{x}, \mathbf{y}, \mathbf{t}, \boldsymbol{\alpha}, \boldsymbol{\beta}, \mathbf{u}} && RC(\mathbf{x}) + FC(\mathbf{y}_o) \\
& \text{s.t.} && \sum_{j \in \delta^-(i)} x_{ijm} = \sum_{j \in \delta^+(i)} x_{jim} \leq 1, && \forall i \in V_e - \{o, s\}, \forall m \in M, \\
& && \sum_{j \in \delta^-(o)} x_{ojm} = \sum_{j \in \delta^+(s)} x_{j sm}, && \forall m \in M, \\
& && \sum_{i \in D^V(j)} \sum_{m \in M} y_{im} = 1, && \forall j \in D, \\
& && \sum_{i \in D_e} y_{im} d_i \leq W, && \forall m \in M, \\
& && \sum_{j \in \delta^+(i)} x_{jim} \geq y_{im}, && \forall i \in D_e, \forall m \in M, \\
& && X_{ijm} = y_{im}, && \forall (i, j) \in A, \forall m \in M, \\
& && t_{jm} \geq t_{im} + \Delta t_{ij} + T (x_{ijm} - 1), && \forall (i, j) \in E_e, \forall m \in M, \\
& && T \geq t_{sm} = t_{om} + \sum_{(i, j) \in E_e} \Delta t_{ij} x_{ijm}, && \forall m \in M, \\
& && t_{jm} \leq a_q + T \alpha_{qijm}, && \forall q \in Q, \forall (m, (i, j)) \in S, \\
& && t_{jm} \geq a_q + T (\alpha_{qijm} - 1), && \forall q \in Q, \forall (m, (i, j)) \in S,
\end{aligned}$$

$$\begin{aligned}
b_q &\leq t_{im} + T \beta_{qijm}, & \forall q \in Q, \forall (m, (i, j)) \in S, \\
b_q &\geq t_{im} + T (\beta_{qijm} - 1), & \forall q \in Q, \forall (m, (i, j)) \in S, \\
u_{qm} &\geq \frac{1}{3}(\alpha_{qijm} + \beta_{qijm} + x_{ijm}) - \frac{2}{3}, & \forall q \in Q, \forall (m, (i, j)) \in S, \\
\sum_{m \in M^a} u_{qm} &\leq B, & \forall q \in Q.
\end{aligned}$$

5 Extended Studies of the MILP

The MILP proposed in Section 4, while exact and polynomial in size, faces limitations when applied to real-world VRP-SA instances. One challenge arises from the discretization of the operational time horizon, which creates a difficult trade-off between model size and performance. Fine granularity leads to a substantial increase in decision variables and constraints, whereas coarse granularity results in holding remote controllers longer than necessary, thereby reducing system capacity. Furthermore, as the system scales, the MILP may quickly become computationally intractable as it is much more complex than typical VRP formulations. In this section, we further explore the MILP formulation from various perspectives, aiming to enhance the model’s comprehensiveness and adaptability. The analysis covered will guide the design of a two-phase tractable algorithm discussed in Section 6.

5.1 The Budget Constraint from the Resource Allocation Perspective

In the MILP, the time horizon of operation is discretized such that the budget constraint can be enforced at any given moment. In practice, however, the benefit of deploying the AV fleet deteriorates as the granularity of discretization increases, because a time interval may have a long non-overlapping sub-interval (e.g., $[t_2, t_5]$ in Figure 3) during which an AV loses the chance to utilize the remote controllers that are indeed available. Therefore, each time interval needs to be short enough. For example, assume the length of time intervals is set to be 30 seconds given that it is a reasonable time for an AV to switch from the automated mode to the remotely-controlled mode, the total number of time intervals in the MILP is as large as 1440 when we have a 12-hour operational window (i.e., $T = 12h$). According to Constraints 12 to 17, the number of variables and constraints in the MILP is multiplied by at least 10^3 to guarantee a relatively precise time discretization. In this section, we formulate an alternative set of constraints from the perspective of *resource allocation* to meet the real-time budget without time discretization.

We override some notations specified in Table 2 for a concise representation. Denote by B the set of remote controllers to be allocated. For example, B can be a quad of remote engineers to assist the AV fleet when AVs are on ordinary roads. Let $w = (w^1, w^2) \in E_e^o$ be an AV-enabled edge in the expanded graph, with w^1 and w^2 representing two end nodes. Define a binary decision variable u_{bmw} for every remote controller $b \in B$, every AV $m \in M^a$, and every edge $w = (i, j) \in E_e^o$. If $u_{bmw} = 1$, the b -th unit is assigned to vehicle m while it is on edge w . The budget is implicitly

satisfied as we only have $|B|$ remote controllers regardless of the assignment. Then, the key idea is to ensure a remote controller b is not assigned to two vehicles simultaneously. More formally, for every two distinct vehicle-edge tuples (m_1, w_1) and (m_2, w_2) in the set $M^a \times E_e^o$ such that $m_1 \neq m_2$, we have $u_{bm_1w_1} + u_{bm_2w_2} \leq 1$ if the following conditions hold:

1. Edge $w_1 = (w_1^1, w_1^2)$ is in the route of vehicle m_1 , which means $x_{m_1w_1} = 1$.
2. Edge $w_2 = (w_2^1, w_2^2)$ is in the route of vehicle m_2 , which means $x_{m_2w_2} = 1$.
3. The time interval of vehicle m_1 traversing edge w_1 overlaps with the time interval of vehicle m_2 traversing edge w_2 .

To describe condition 3 rigorously, we further define a binary decision variable $\alpha(w_1, w_2, m_1, m_2)$ for every pair of vehicle-edge tuples in the set $S^2 = \{((m_1, w_1), (m_2, w_2)) \mid m_1 \neq m_2, m_1, m_2 \in M^a, w_1, w_2 \in E_e^o\}$. If and only if $\alpha(w_1, w_2, m_1, m_2) = 1$, the timestamp of vehicle m_1 entering edge w_1 is earlier than or equal to the timestamp of vehicle m_2 exiting edge w_2 , which means $t_{w_1^1m_1} \leq t_{w_2^2m_2}$. By analogy, we define $\beta(w_1, w_2, m_1, m_2)$ to indicate whether the timestamp of vehicle m_1 exiting edge w_1 is later than or equal to the timestamp of vehicle m_2 entering edge w_2 , namely $t_{w_2^1m_2} \leq t_{w_1^2m_1}$. To capture such sufficient and necessary conditions, we can formulate Constraints 18 to 21 for every element in S^2 .

$$t_{w_2^2m_2} \leq t_{w_1^1m_1} + T \alpha(w_1, w_2, m_1, m_2), \quad (18)$$

$$t_{w_2^2m_2} \geq t_{w_1^1m_1} + T (\alpha(w_1, w_2, m_1, m_2) - 1), \quad (19)$$

$$t_{w_1^2m_1} \leq t_{w_2^1m_2} + T \beta(w_1, w_2, m_1, m_2), \quad (20)$$

$$t_{w_1^2m_1} \geq t_{w_2^1m_2} + T (\beta(w_1, w_2, m_1, m_2) - 1). \quad (21)$$

Next, for every $b \in B$ and every element in S^2 , we can formulate Constraint 22 to describe the sufficient condition for $u_{bm_1w_1} + u_{bm_2w_2} \leq 1$. Finally, the set of Constraints 18 to 22 is a replacement for Constraints 12 to 17 for a complete MILP.

$$u_{bm_1w_1} + u_{bm_2w_2} \leq \frac{11}{4} - \frac{1}{4}(x_{m_1w_1} + x_{m_2w_2} + \alpha(w_1, w_2, m_1, m_2) + \beta(w_1, w_2, m_1, m_2)). \quad (22)$$

Discarding time discretization is not always beneficial from the complexity point of view. The number of decision variables and the number of constraints in the new MILP are $\mathcal{O}(k |S^2| |B|)$, which may be more complex than that of the first MILP when the input is a huge road network because $|S^2|$ is $\mathcal{O}(|S|^2)$. In practice, however, we cannot conclude which formulation is superior to the other unless a specific instance is given.

5.2 Size Reduction of the MILP

The MILP proposed in Section 4 has three folds of extra complexity compared to a basic VRP formulation: (1) The vehicle routing is modeled in a k -layer expanded graph. (2) Each layer is

a real-world road network instead of the metric closure constructed on the set of customers. (3) A set of constraints, similar to those found in job scheduling problems, is added to the routing component in order to meet the budget of available remote controllers for real-time AV operations. Hence, in this section, we discuss two pre-processing heuristics to reduce the size of the MILP while keeping the sub-optimality gap small in general.

Heuristic 1: Reducing the Number of Layers in the Expanded Graph

In Proposition 4.3, we concluded that the number of layers in the expanded graph has to be at least k to guarantee the optimality of the MILP, where k is the maximum number of customers a vehicle can potentially serve under any circumstances and the upper bound of k is the total number of customers in the instance. However, in practice, most urban networks follow a grid-like structure and consist predominantly of two-way roads, which is very different than the pathological example used to prove Lemma 4.2. For more details, refer to Figure 10 in Appendix A. Moreover, the customers and the depot are spatially distributed more uniformly, resulting in less intersecting minimum-cost paths between them. In many of these real-world instances, the chance of a vehicle visiting a single intersection very frequently is significantly reduced. In other words, an optimal vehicle route may pass a single intersection significantly fewer times than k . Example 5.1 illustrates such a realistic instance.

Example 5.1. *An undirected road network is shown in Figure 4a. Every node represents an intersection and every edge represents a road segment. The sky-blue node represents the depot and the light-purple nodes represent customers. The routing cost on an edge is proportional to its length. Suppose only one vehicle with unlimited capacity is available in the system. The optimal route can be obtained by observation, which is highlighted in Figure 4b. Notice that there are 6 customers but only node 2 and node 8 are visited twice.*

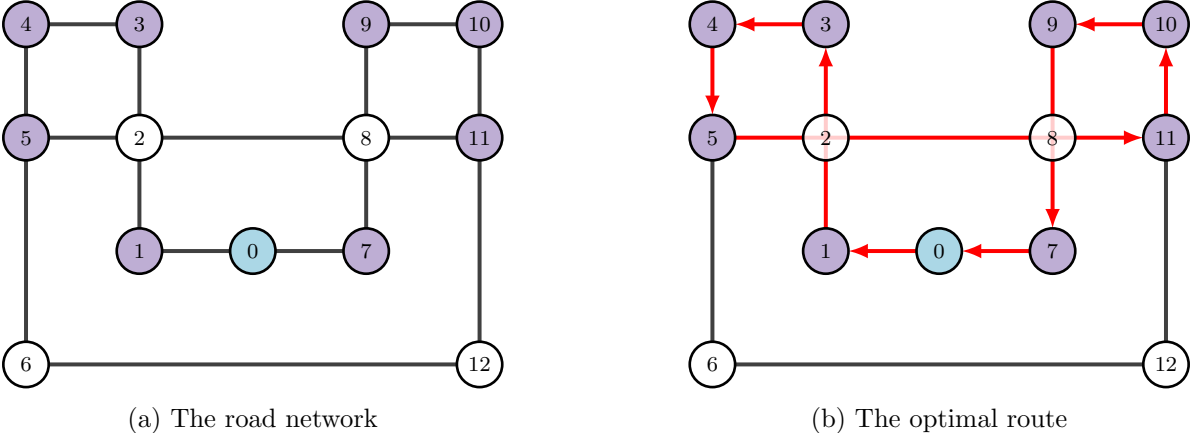


Figure 4: A realistic VRP instance in the real-world road network

Hence, it is justified to reduce the number of layers in the expanded graph from k to a smaller integer \bar{k} . Nevertheless, a naive reduction may cause a highly sub-optimal solution or even make

the MILP infeasible because the transition Constraint 9 forces every vehicle to move one layer up every time it serves a customer except that it is already on the topmost layer. When $\bar{k} \ll k$, any vehicle tends to move to the topmost layer as soon as possible even though the route does not intersect with itself in serving the first few customers. In Example 5.1, a 3-layer expanded graph is sufficient as no node is visited more than twice in the optimal solution shown in Figure 4b, but the existence of Constraint 9 excludes this true optimal solution from the feasible space, resulting in a sub-optimal solution that re-routes to edge (5, 6) instead of edge (5, 2).

To circumvent this disadvantage, we re-design the transition constraint by replacing Constraint 9 with Constraint 23. Due to the inequality, a transition of layers after serving a customer is no longer compulsory but optional. The transition only occurs if it leads to a better solution. Despite the improvement by this soft transition constraint, an “optimal” solution given by the updated MILP can still deviate from a true optimum of the problem if \bar{k} is too small for a given instance. One strategy is to solve the MILP with $\bar{k} = 1$ and iteratively increase \bar{k} until the optimal value converges or the reduced cost is less than a small threshold.

$$x_{ijm} \leq y_{im}, \quad \forall (i, j) \in A, \forall m \in M. \quad (23)$$

Heuristic 2: Pre-Prune the Road Network

The network pre-pruning heuristic is motivated by Proposition 5.1 presented in the work by Rodriguez-Pereira et al. [39]. Recall that the VRP-SA generalizes from the STSP, where both the depot and customers are regarded as required nodes. Intuitively, if an edge is part of an optimal solution to a VRP-SA instance, it is highly probable to appear in a minimum-cost path between customers or in a path that utilizes remote controllers for the least amount of time. Therefore, it is justifiable to pre-prune the input road network before we construct the expanded graph.

The pre-processing steps are as follows: (1) Compute the minimum-cost paths between any pair of nodes in the set of customers and the depot. Denote by P_1 and V_1 the set of all edges and nodes used in those paths, respectively. (2) Compute the paths for any pair of nodes in the set of customers and the depot such that each path utilizes remote controllers for the shortest duration. Denote by P_2 and V_2 the set of edges and nodes used in those paths, respectively. (3) Identify all other AV-enabled strongly connected components that are connected to P_1 and P_2 . Denote by P_3 and V_3 the set of all edges and nodes used in such components, respectively. (4) Remove all edges that are not in $P_1 \cup P_2 \cup P_3$ and all nodes that are not in $V_1 \cup V_2 \cup V_3$. The resulting sparse subgraph $G_s = (V_1 \cup V_2 \cup V_3, P_1 \cup P_2 \cup P_3)$ replaces the original network G and is used to construct the expanded graph G_e .

Proposition 5.1. *In any optimal solution to a given Steiner traveling salesmen problem instance, all edges used belong to some minimum-cost paths in the network connecting two required nodes.*

6 A Two-Phase Tractable Algorithm

As discussed in Section 5.2, the size complexity of the original MILP renders it computationally intractable for any practical instances in the real world. Even with the application of the aforementioned size reduction heuristics in Section 5.2, directly solving the VRP-SA using the most powerful MILP solver remains challenging. Therefore, in this section, we develop a two-phase algorithm to efficiently find high-quality solutions to medium-size VRP-SA instances with up to 100 customers and 2000 edges in the road network.

In phase 1, given any instance \mathcal{I}_0 of the VRP-SA, we create an instance \mathcal{I}_1 of the *Heterogeneous Vehicle Routing Problem with Fixed Costs and Vehicle-Dependent Routing Cost (H-VRP-FD)* by removing the budget constraint of remote controllers. Naturally, the optimal value of \mathcal{I}_1 is a lower bound for that of \mathcal{I}_0 . Then, we solve \mathcal{I}_1 efficiently to obtain a near-optimal solution. The exact optimum can be also pursued if the instance size permits. Currently, the state-of-the-art exact and heuristic approaches for this VRP variant are due to Baldacci and Mingozzi [2] and Vidal et al. [46], respectively.

By decoding the solution to \mathcal{I}_1 , we can derive all routes of vehicles dispatched. Denote by \tilde{X} the set of routes of the HDV fleet, and by X the set of routes of the AV fleet. In particular, $\tilde{X} = \{X(m) \mid \forall m \in \overline{M}^h\}$ and $X = \{X(m) \mid \forall m \in \overline{M}^a\}$, where $X(m)$ is the *route* of vehicle m represented as a sequence of road intersections visited, and \overline{M}^h (\overline{M}^a) is the set of all dispatched (HDVs) AVs. Each $X(m)$ can be used to infer the *routing schedule* $\mathcal{T}(m)$, which contains the timestamps of the vehicle visiting intersections on the route. All vehicle departure times are set to be zero. Denote by $\tilde{\mathcal{T}} = \{\mathcal{T}(m) \mid m \in \overline{M}^h\}$ the set of routing schedules of dispatched HDVs, and by $\mathcal{T} = \{\mathcal{T}(m) \mid m \in \overline{M}^a\}$ the set of routing schedules of dispatched AVs.

In phase 2, we check whether the set of routing schedules \mathcal{T} is feasible with respect to the budget of remote controllers, and recover the solution feasibility if necessary. Recall that $\tilde{\mathcal{T}}$ does not impact the feasibility of the solution to \mathcal{I}_0 since HDVs do not require assistance from remote controllers. However, the schedules \mathcal{T} for AVs might be infeasible. For any two consecutive timestamps, t_{im} and t_{jm} , in the routing schedule $\mathcal{T}(m)$, we can determine whether AV m occupies a remote controller depending on the type of edge (i, j) . This enables us to efficiently verify whether (X, \mathcal{T}) violates the budget constraint over certain time intervals. If the budget is not exceeded, then $(\tilde{X} \cup X, \tilde{\mathcal{T}} \cup \mathcal{T})$ is a feasible and therefore an optimal solution to \mathcal{I}_0 . On the contrary, if the budget is exceeded, we solve a *feasibility recovering sub-problem (FRP)* to find a near-optimal solution $(\tilde{X} \cup X^*, \tilde{\mathcal{T}} \cup \mathcal{T}^*)$ to \mathcal{I}_0 , where (X^*, \mathcal{T}^*) are the updated AV routes and their schedules. Two families of FRP based on *re-scheduling* strategy and *re-routing* strategy will be discussed in Section 6.1 and Section 6.2, respectively.

The two-phase algorithmic pipeline is detailed in Algorithm 1, with the sub-routines in Line 3 and Line 6 elaborated later. It is important to note that neither the re-scheduling FRP nor re-routing FRP guarantees a complete recovery of the solution feasibility for $(\mathcal{X}, \mathcal{T})$. In the worst case, it may be necessary to replace some AVs with HDVs to serve certain customers and avoid

exceeding the budget. If no additional HDVs are available in the system, the instance will be deemed infeasible.

Algorithm 1 The Two-Phase Algorithmic Pipeline to Solve the VRP-SA

Input: A VRP-SA instance \mathcal{I}_0

Output: Feasible vehicle routes are schedules $(\tilde{X} \cup X^*, \tilde{\mathcal{T}} \cup \mathcal{T}^*)$

- 1: Construct an instance \mathcal{I}_1 of the H-VRP-FD based on \mathcal{I}_0 ,
 - 2: $(\tilde{X}, X, \tilde{\mathcal{T}}, \mathcal{T}) \leftarrow \text{HVRPPDSolver}(\mathcal{I}_1)$
 - 3: $\mathcal{T}^* \leftarrow \text{ReSchedulingFRPSolver}(\mathcal{T})$
 - 4: $X^* \leftarrow X$
 - 5: **if** $\mathcal{T}^* = \emptyset$ **then**
 - 6: $(\bar{D}, X^*, \mathcal{T}^*) \leftarrow \text{ReRoutingFRPSolver}(X, \mathcal{T})$
 - 7: **if** $\bar{D} \neq \emptyset$ **then**
 - 8: $\tilde{X}_{\bar{D}} \leftarrow \text{CVRPSolver}(\bar{D})$
 - 9: $\tilde{X} \leftarrow \tilde{X} \cup \tilde{X}_{\bar{D}}$
 - 10: **end if**
 - 11: **end if**
-

Theoretically, Algorithm 1 may still fail to return a feasible solution even though \mathcal{I}_0 is indeed feasible. This limitation stems from the inherent nature of the relax-then-recover framework, which decomposes customer assignment and sequencing without incorporating a mechanism to iteratively explore the entire search space of the VRP-SA. Consequently, it may miss feasible solutions that require more nuanced exploration. However, we hypothesize that, under realistic conditions in the real world, a VRP-SA instance is very likely to be infeasible if Algorithm 1 fails to find a feasible solution.

6.1 The Re-Scheduling Feasibility Recovering Sub-Problem

One strategy to recover the feasibility of (X, \mathcal{T}) is to re-schedule \mathcal{T} while keeping the set of routes X unchanged. For each routing schedule $\mathcal{T}(m)$, we can extract a subset of timestamps called *transition timestamps*, at which an AV switches between an AV-enabled road and an ordinary road. All road segments of the same type traveled between any two consecutive transition timestamps can be merged into a *sub-route*. We observe that, the departure time is not necessarily zero for every vehicle in the optimal solution to the VRP-SA, as the departure delay of some vehicles may benefit the system by adding more feasibility to the temporal space of the problem. In another word, the routing schedule of every AV, as a whole, can potentially be shifted forward in time to avoid budget violations, provided the vehicle’s return time is earlier than the end of the operation horizon T .

Figure 5 illustrates this re-scheduling process for a small instance with two AVs and a single remote controller. In the figure, each strip represents a time interval during which an AV occupies a remote controller on an ordinary sub-route. The original schedules are infeasible due to overlapping strips between vehicles m_1 and m_2 . If we delay the departure of vehicle m_2 by δ , highlighted in purple strips, the schedules become feasible. This rescheduling does not increase the overall cost, as a departure delay does not inherently affect the operation negatively. In general, the *re-scheduling*

FRP takes \mathcal{T} as the input and aims to find a feasible shift of the routing schedule $\mathcal{T}(m)$ for every dispatched vehicle m , such that the updated schedules \mathcal{T}^* are feasible to \mathcal{I}_0 .

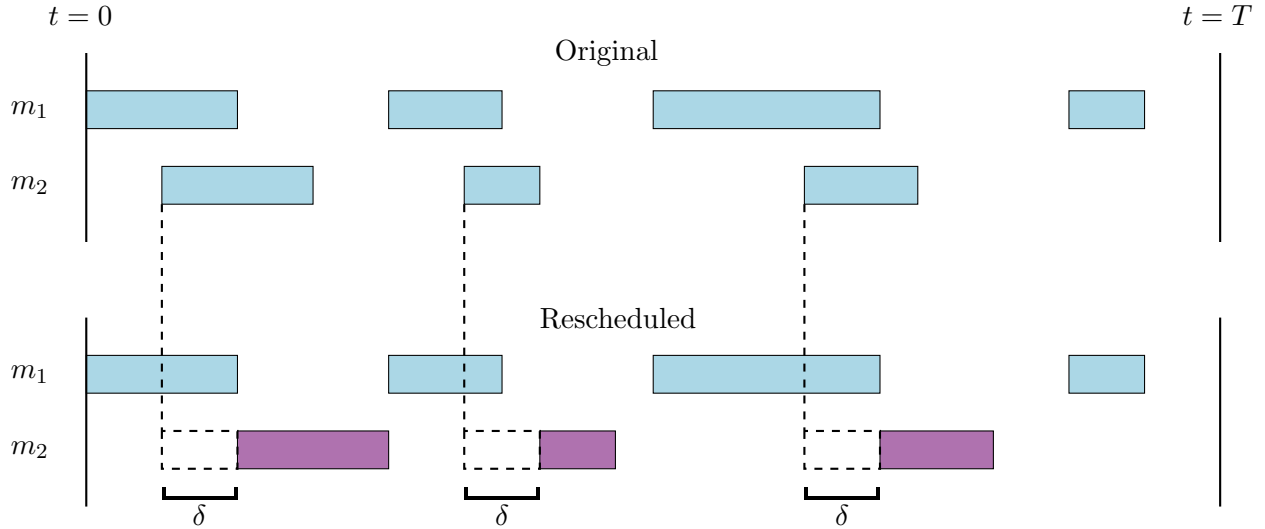


Figure 5: The illustration of the re-scheduling FRP with fixed travel time

The re-scheduling FRP is a feasibility problem that can be exactly modeled by an MILP without an objective function, referred to as the *re-scheduling MILP*, which will be elaborated upon later. Notably, the formulation of this re-scheduling MILP resembles the constraints in Section 5.1 which handled the budget constraint from a resource allocation perspective.

Denote by $R = R^a \cup R^o$ the set of sub-routes, where R^a is the subset of AV-enabled sub-routes and R^o is the subset of ordinary sub-routes. Denote by Δt_r the travel time in sub-route r . Define a continuous decision variable $\bar{t}_m \in [0, T]$ as the re-scheduled departure time for each dispatched AV $m \in \bar{M}^a$. Furthermore, define two continuous decision variables $t_r^1 \in [0, T]$ and $t_r^2 \in [0, T]$ as the timestamp of the associated vehicle entering and exiting sub-route r , respectively. Then, the consistency among timestamps can be captured by Constraints 24 and 25, where $r' \prec r$ means sub-route r' is traversed earlier than sub-route r on the same route.

$$t_r^1 = \bar{t}_m + \sum_{r': r' \prec r} \Delta t_{r'}, \quad \forall r \in R, \quad (24)$$

$$t_r^2 = t_r^1 + \Delta t_r, \quad \forall r \in R. \quad (25)$$

Define a binary variable $u_{br} \in \{0, 1\}$ for every remote controller $b \in B$ and every ordinary sub-route $r \in R^o$. If $u_{br} = 1$, the b -th controller is assigned to the sub-route r . Constraint 26 regulates the unique assignment of one remote controller to a single ordinary sub-route.

$$\sum_{b \in B} u_{br} = 1, \quad \forall r \in R^o. \quad (26)$$

Define a set $R^2 = \{(r_1, r_2) \mid r_1, r_2 \in R^o, r_1 \not\parallel r_2\}$, where $r_1 \not\parallel r_2$ means sub-routes r_1 and r_2 are not on the same route. For each pair of sub-routes in R^2 , define a binary decision variable $\alpha(r_1, r_2)$. If and only if $\alpha(r_1, r_2) = 1$, the start time of sub-route r_1 is earlier than or equal to the end time of sub-route r_2 , which means $t_{r_1}^1 \leq t_{r_2}^2$. By analogy, we define $\beta(r_1, r_2)$ to indicate whether the end time of sub-route r_1 is later than or equal to the start time of sub-route r_2 , namely $t_{r_2}^1 \leq t_{r_1}^2$. To capture these sufficient and necessary conditions, we formulate Constraints 27 to 30.

$$t_{r_2}^2 \leq t_{r_1}^1 + T \alpha(r_1, r_2), \quad \forall (r_1, r_2) \in R^2, \quad (27)$$

$$t_{r_2}^2 \geq t_{r_1}^1 + T (\alpha(r_1, r_2) - 1), \quad \forall (r_1, r_2) \in R^2, \quad (28)$$

$$t_{r_1}^2 \leq t_{r_2}^1 + T \beta(r_1, r_2), \quad \forall (r_1, r_2) \in R^2, \quad (29)$$

$$t_{r_1}^2 \geq t_{r_2}^1 + T (\beta(r_1, r_2) - 1), \quad \forall (r_1, r_2) \in R^2. \quad (30)$$

Then, we can formulate Constraint 31 to avoid a remote controller being assigned to two ordinary sub-routes simultaneously. Overall, all the constraints of the re-scheduling MILP are listed from 24 to 31.

$$u_{br_1} + u_{br_2} \leq \frac{5}{2} - \frac{1}{2}(\alpha(r_1, r_2) + \beta(r_1, r_2)), \quad \forall (r_1, r_2) \in R^2. \quad (31)$$

One may notice that the re-scheduling FRP is also an NP-hard problem, and the core constraints from 27 to 31 in the re-scheduling MILP exhibit structural similarity to the highly complex constraints discussed in Section 5.1. In practice, however, the re-scheduling FRP can be solved much more efficiently as the total number of sub-routes is much less than the total number of edges in the network. It is justified because AV-enabled roads tend to form a skeleton within the network as smart infrastructure develops, leading to less frequent transitions between AV-enabled road segments and ordinary road segments along a vehicle route.

Building on the concept of flexible departure times aforementioned, we further explore a scenario where the travel times of AVs on each road segment is also flexible. This unlocks an even larger feasible space for both the VRP-SA and the re-scheduling FRP. Detailed discussions are provided in Appendix B.

6.2 The Re-Routing Feasibility Recovering Sub-Problem

In this section, we discuss the re-routing strategy to recover the feasibility of (X, \mathcal{T}) . Unlike the re-scheduling FRP, the re-routing FRP takes both X and \mathcal{T} as the input and aims to find a feasible set of vehicle routes X^* along with the updated routing schedules \mathcal{T}^* . Importantly, the customer-to-vehicle assignment remains unchanged, with adjustments made only within individual vehicle routes.

The re-routing FRP is an optimization problem with the objective of minimizing the additional cost incurred by route perturbation. It generalizes the re-scheduling FRP, as perturbing a route includes the special case of adjusting only the departure time (or all timestamps under the flexible

travel time assumption discussed in Appendix B). Due to its complexity, finding an exact solution is challenging. Therefore, we develop an iterative algorithm based on the *ruin-and-recreate* principle and a *route priority heuristic* to solve it approximately.

First of all, we convert (X, \mathcal{T}) to a priority queue, where the priority of a route $X(m)$ is determined by its value $v(m)$, as defined in Equation 32. Two cost adjustment factors $\eta_1 < 1$ and $\eta_2 > 1$ that are defined in Section 3 play a key role here. Let $c^1(m)$ and $c^2(m)$ represent the total routing costs of AV-enabled roads and ordinary roads, respectively, in route $X(m)$. Routes that better utilize AV-enabled roads are more valuable compared to HDV routes. We also initialize X^* and \mathcal{T}^* as two empty containers to store feasible routes and their routing schedules.

$$v(m) = \frac{1 - \eta_1}{\eta_1} c^1(m) + \frac{1 - \eta_2}{\eta_2} c^2(m) \quad (32)$$

Then, in each iteration, the algorithm pops the route $X(m)$ with the highest value from the priority queue and examines whether its routing schedule $\mathcal{T}(m)$, when combined with any other existing routing schedules in \mathcal{T}^* , violates the budget constraint at a certain point in time. If no violation occurs, $X(m)$ and $\mathcal{T}(m)$ are moved to the feasible containers, and the algorithm proceeds to the next iteration. If a violation is detected, the current route $X(m)$ is “ruined”, and the algorithm attempts to recreate a new route $X^*(m)$ such that the following two constraints are satisfied: (1) Vehicle m avoids ordinary road segments when the budget is exhausted or exceeded given the schedules of remaining routes. (2) The return time of vehicle m is less than the end time of operation. The re-creation process is essentially solving a *Constrained Steiner Traveling Salesman Problem* (CSTSP). It takes as input the original network G , the subset of customers $D(m)$ served by the current route $X(m)$, the operational end time T , and the feasible routing schedules \mathcal{T}^* , and output a new feasible route $X^*(m)$ or report that no solution exists. Whenever the algorithm fails to recreate a feasible route cheaper than dispatching an HDV, it adds $D(m)$ to the set of unserved customers \bar{D} .

The CSTSP, a crucial component of the algorithm, can be modeled similarly to the VRP-SA discussed in Section 4, but with substantially reduced complexity. We first apply the size reduction heuristics from Section 5.2 and construct an expanded graph $G_e(m)$ following the steps in Section 4. The resulting graph is considerably smaller than G_e for the full VRP-SA because the graph pre-pruning removes more edges given that $|D(m)| < |D|$. We then formulate a similar MILP, called *re-routing MILP*, based on $G_e(m)$. The primary modifications are highlighted as follows while further details are provided in Appendix C.

1. Since the problem involves only one vehicle route, which must be dispatched, we eliminate the fixed cost component from the objective function and remove the vehicle index from all decision variables.
2. Manual time discretization is unnecessary. Instead, we construct the set of non-overlapping time intervals by partitioning the operational time horizon $[0, T]$ based on the timestamps in the set $\{(i, j) \mid i, j \in \mathcal{T}' \cup \{T\}\}$, where $\mathcal{T}' = \bigcup_{\mathcal{T}(m) \in \mathcal{T}^*} \mathcal{T}(m)$ represents a merged set of

Algorithm 2 The re-routing FRP solver

Input: Graph G , AV routes and schedules (X, \mathcal{T}) , End time of operation T
Output: Updated AV routes and schedules (X^*, \mathcal{T}^*) , Unserved customers \bar{D}

- 1: $(X, \mathcal{T}) \leftarrow \text{PriorityQueueByValues}(X, \mathcal{T})$
- 2: Initialize $(X^*, \mathcal{T}^*) = (\emptyset, \emptyset)$
- 3: **while** $(X, \mathcal{T}) \neq \emptyset$ **do**
- 4: $(X(m), \mathcal{T}(m)) \leftarrow (X, \mathcal{T}).\text{dequeue}()$
- 5: **if** $\mathcal{T}^* \cup \{\mathcal{T}(m)\}$ does not violate budget at any time **then**
- 6: $X^* \leftarrow X^* \cup \{X(m)\}$
- 7: $\mathcal{T}^* \leftarrow \mathcal{T}^* \cup \{\mathcal{T}(m)\}$
- 8: **continue**
- 9: **end if**
- 10: $D(m) \leftarrow \text{ExtractCustomers}(X(m))$
- 11: $G_s(m) \leftarrow \text{GraphPruner}(G, D(m))$
- 12: $G_e(m) \leftarrow \text{GraphExpander}(G_s(m))$
- 13: $(X^*(m), \mathcal{T}^*(m)) \leftarrow \text{ReRoutingMILPSolver}(G_e(m), D(m), \mathcal{T}^*, T)$
- 14: $UB \leftarrow \text{TSPSolver}(D(m))$
- 15: **if** $X^*(m) = \emptyset$ or $X^*(m)$ is more expansive than UB **then**
- 16: $\bar{D} \leftarrow \bar{D} \cup D(m)$
- 17: **else**
- 18: $X^* \leftarrow X^* \cup \{X^*(m)\}$
- 19: $\mathcal{T}^* \leftarrow \mathcal{T}^* \cup \{\mathcal{T}^*(m)\}$
- 20: **end if**
- 21: **end while**

timestamps from the current feasible routing schedules \mathcal{T}^* .

Overall, Algorithm 2 provides a complete pseudo-code for the re-routing FRP solver. As aforementioned, the order of iteration of routes is not arbitrary but depends on the route priority heuristic. Routes with higher values are less likely to be perturbed or replaced, which guides the algorithm towards solutions with lower total routing costs. Additionally, if the algorithm terminates with a non-empty set \bar{D} , it indicates that the feasibility of (X, \mathcal{T}) has not been fully recovered. This outcome could be due to one of the following reasons: (1) the re-routing FRP is infeasible with the current customer-to-vehicle assignments, or (2) the re-routing FRP is feasible but the algorithm fails to find a feasible solution. Nevertheless, the algorithm is devised to recover the feasibility to the greatest extent possible.

7 Numerical Experiments

In this section, we construct a tailored set of instances for the VRP-SA and solve them using Algorithm 1 described in Section 6. The results (1) validate the effectiveness and efficiency of the proposed two-phase algorithm and (2) illustrate how variations in input parameters influence both the problem structure and the corresponding solutions.

7.1 VRP-SA Instances

We construct 23 VRP-SA instances, each based on a CVRP instance from the benchmark dataset P described by Augerat [1]. The number of customers in these CVRP instances ranges from 16 to 101. Each CVRP instance provides the following inputs: the coordinates of the depot and customers in a 2D Euclidean space, customer demands, and a uniform vehicle capacity. These inputs are directly adopted for the corresponding VRP-SA instances.

To accommodate the additional attributes of the VRP-SA, we construct an underlying road network for each CVRP instance based on the coordinates of all nodes. The process is as follows: (1) Draw a rectangular bounding box such that the farthest nodes are positioned along its boundary. (2) Construct a primary grid by equally dividing the bounding box along both the x- and y-axes, with two hyperparameters, g_x and g_y , determining the number of divisions in each direction. Unless otherwise specified, we set $g_x = g_y = 5$ in the following experiments. This grid serves as the skeleton of the underlying road network, where all road segments are AV-enabled. (3) Within each cell of the primary grid, we construct a local grid, where each customer within the cell is placed precisely at an intersection. All road segments within the local grids are ordinary roads. Figure 6 illustrates the underlying road network of instance P-n40-k5. The design aims to mimic real-world semi-autonomous environments, where infrastructure upgrades to support AVs are prioritized on primary avenues in cities.

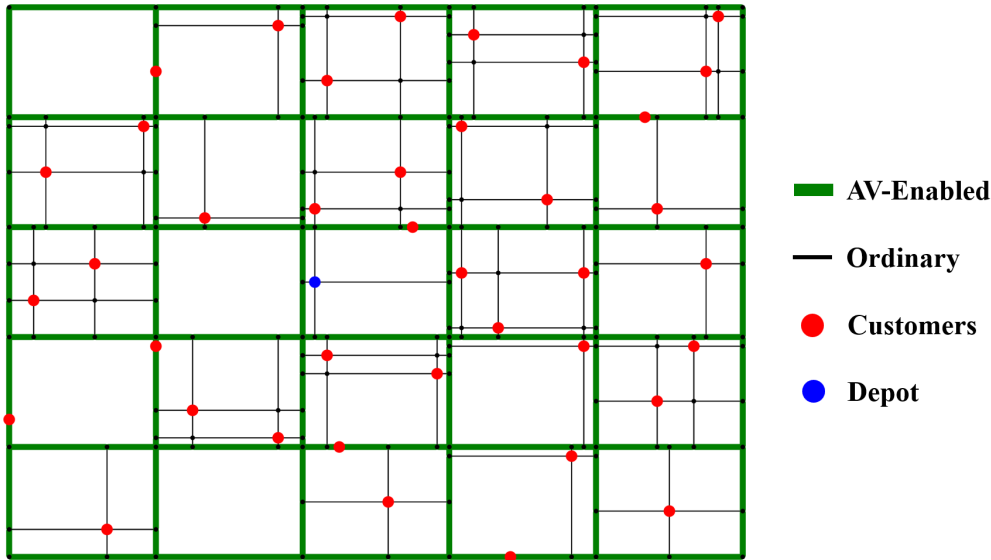


Figure 6: The underlying road network of P-n40-k5

As assumed in Section 3, the unit routing cost of an AV on the primary grid is lower than that of an HDV. Conversely, it is more cost-demanding for an AV to travel on local grids than an HDV. For HDVs, the routing cost on any edge in the road network is equal to the edge length. For AVs, the routing cost on an edge in the primary grid is given by η_1 times the edge length, while on local grids, it is η_2 times the edge length. In the following experiments, we set $\eta_1 = 0.5$ and $\eta_2 = 1.2$ if

not otherwise specified.

To guarantee that all VRP-SA instances are feasible, which simplifies the analysis of experimental results, we set the size of the AV fleet, $|M^a|$, and the HDV fleet, $|M^h|$, in each VRP-SA instance to match the number of vehicles used in the optimal solution of the corresponding CVRP instance. To avoid over-dispatching, we assign an equal fixed dispatch cost (e.g., 1) to all vehicles.

For each VRP-SA instance, we define the operation end time as $T = T_{factor} \cdot \bar{T}$, where \bar{T} is the maximum return time of all vehicles in the optimal solution to the CVRP instance with only HDVs deployed. The parameter $T_{factor} \in [1, \infty]$ serves as a time-horizon factor that controls the relative tightness of the operation time window. Note that travel time and routing cost are used interchangeably since the VRP instances in this section are synthetic. In the following experiments, we set $T_{factor} = 1.2$, unless otherwise specified.

Finally, we introduce a budget B that determines the number of remote controllers available to assist AVs on ordinary local grids. In the experiments, we set $B = \max(1, \text{round}(\frac{|M^a|}{3}))$ unless otherwise specified, which roughly corresponds to one-third of the AV fleet size in each VRP-SA instance. This percentage-based approach provides more flexibility, as the minimum number of dispatched vehicles varies significantly across instances.

7.2 Algorithm Settings

Strictly speaking, the algorithm must solve an H-VRP-PD in Phase 1, as shown in Line 2 of Algorithm 1, before proceeding to Phase 2 for re-scheduling or re-routing. This initial step is computationally intensive. From an experimental standpoint, we simplify Phase 1 by solving a CVRP with only the AV fleet deployed, under the same settings. While this solution is suboptimal compared to that for the H-VRP-PD, it reduces computational demands. In practice, the algorithm’s performance can be further improved by exactly solving the H-VRP-PD, which would provide a true lower bound for the VRP-SA. For the CVRP, we use the state-of-the-art solver *HGS-CVRP* developed by Vidal [45]. The TSP solver used in Line 14 of Algorithm 2 is from Google OR-Tools. All other MILPs are solved using Gurobi 10.0.1, with several hyperparameters fine-tuned for each instance. Specifically, the `TimeLimit` for all Gurobi solvers is set to 300 seconds to enforce termination. Unless otherwise specified, the number of layers k in the expanded graph is set to 2.

7.3 Baseline Results

For each VRP-SA instance, we denote f^P as the routing cost obtained using the proposed algorithm with the re-routing priority heuristic, and $f^{\bar{P}}$ as the routing cost obtained with a random re-routing order. Additionally, we denote f_1 as the near-optimal routing cost for the CVRP instance with only the AV fleet deployed, as obtained in Phase 1, and f_2 as the near-optimal routing cost for the CVRP instance with only the HDV fleet deployed, representing the cost without exploiting AVs at all. To account for variability due to instance sizes, we report the *routing cost ratios* f_2/f_1 , f^P/f_1 , and $f^{\bar{P}}/f_1$, instead of the absolute routing costs, for all instances ranging from 0 to 22. Given an

instance, the quantity $f_2/f_1 - 1$ approximately measures the percentage increase in routing cost when operating in a non-autonomous environment compared to a semi-autonomous environment with unlimited remote controllers. Similarly, $f^P/f_1 - 1$ or $f^{\bar{P}}/f_1 - 1$ quantify the percentage increase in routing cost under a limited budget of remote controllers.

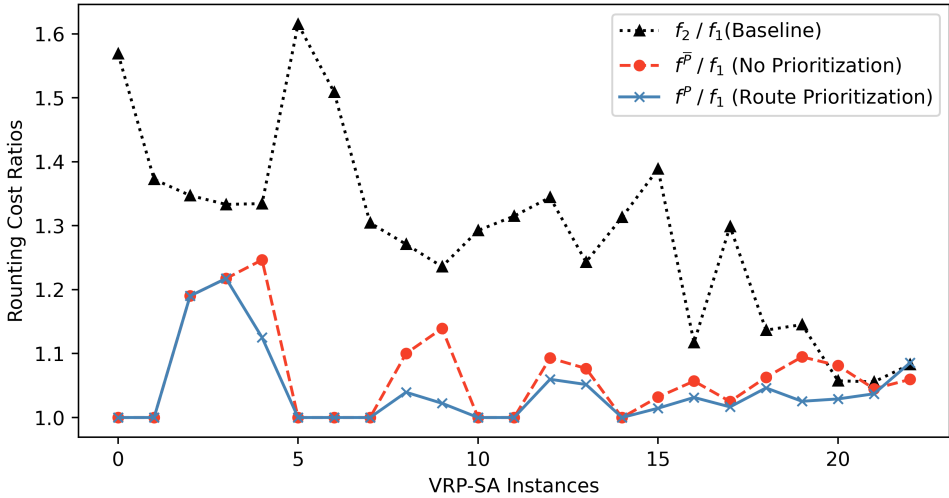


Figure 7: Routing cost ratios in different VRP-SA instances

As shown in Figure 7, the proposed algorithm with only a random re-routing order generally yields lower routing cost ratios than the baseline with only the HDV fleet deployed (i.e., no AVs involved), except for instance 20. The greatest cost reduction is over 37.5% in instance 5. If the re-routing priority heuristic is enabled, the algorithm performs even better in most cases, except for instance 22. Moreover, the algorithm successfully re-schedules the vehicle routes obtained in Phase 1 to feasibility without evoking the re-routing component in 8 out of 23 instances (i.e., instances 0, 1, 5, 6, 7, 10, 11, and 14), which is advantageous as it results in zero additional routing cost. More numerical details are available in Appendix C.

We also observe two secondary patterns from the results: (1) As instance size increases, f_2/f_1 tends to decrease. Since the instances in Figure 7 are ordered first by the number of customers and then by the number of available vehicles, this trend is expected. The number of divisions, g_x and g_y , in the primary grid remains fixed across all instances, leading to a higher customer density within each grid cell for larger instances. Consequently, AV-enabled roads become relatively “sparser” in larger instances, diminishing the advantage of dispatching AVs. The effect of AV-enabled road density is further examined in Section 7.4. (2) In instances where f_2/f_1 is relatively low (e.g., instances 2, 3, 4, 8, 9, 13, and 16), $f^{\bar{P}}/f_1$ or f^P/f_1 tend to be relatively high, and vice versa. This pattern follows a similar rationale as the first. When f_2/f_1 is low, AVs face greater difficulty in effectively leveraging AV-enabled roads, making re-routing less feasible and increasing its cost.

7.4 Sensitivity Analysis of Input Parameters

We conduct a series of experiments by varying the budgets and time-horizon factors while keeping other input parameters at their default values. Specifically, we set $B = \max(2, \text{round}(|M^a| \cdot B_{factor}))$ with $B_{factor} = (1/3, 1/2, 2/3)$ and $T_{factor} = (1.0, 1.1, 1.2, 1.3, 1.4, 1.5)$. The results shown in Figure 8a and Figure 8b are the average values across all 23 instances. As the budget and the tightness of the operational time horizon increase, the routing cost ratio f^P/f_1 decreases to as low as 1.006, resulting in a significant cost reduction of up to 22%. Theoretically, an instance with a looser time-horizon factor should save more cost than that with a tighter time-horizon factor. The observed discrepancy for the results of $(B_{factor}, T_{factor}) = (1/2, 1.4)$ is attributed to the indeterministic behavior in the Gurobi solver under the parameter setting concerning the maximum running time.

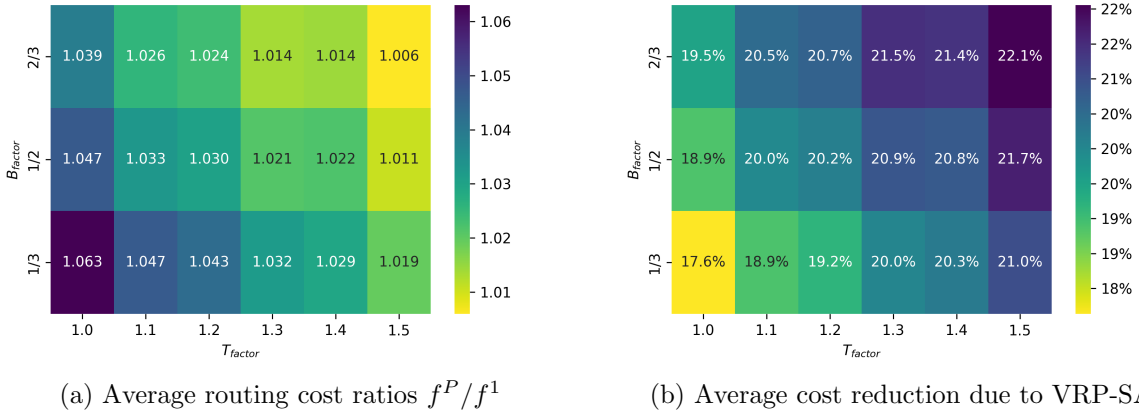


Figure 8: Changing budget and the tightness of operational time horizon

We also vary the number of divisions g_x and g_y from 3 to 7 in the primary grid, while keeping other input parameters at their default values. Figure 9 shows the *inverse routing cost ratio* f_1/f_2 , where the ratio upper bound is 1.0, representing the cost of dispatching only HDVs. According to the result, it becomes increasingly advantageous to replace HDVs with AVs in networks with denser AV-enabled roads. Moreover, ratio f^P/f_2 closely follows the trend of f_1/f_2 , indicating that the proposed model and algorithm effectively leverage the increased density of AV-enabled roads to reduce routing costs. The density of AV-enabled roads serves as a metric for quantifying the degree of transition from a current environment to a fully autonomous one. Interestingly, the results reveal a two-stage pattern in this trend. In stage one (i.e., $g_x = g_y \leq 5$) when the density is relatively low, the gap between f^P/f_1 and f_1/f_2 widens as the density increases. This is due to the budget constraint of remote controllers, which limits AVs from using all available road segments in routing. In stage two (i.e., $g_x = g_y \geq 5$) when the density surpasses a certain threshold, the gap starts to narrow as the density increases further. This is because the AV fleet relies less on remote control when most ordinary roads are upgraded to AV-enabled, thus diminishing the impact of the budget constraint on both re-scheduling and re-routing. This two-stage pattern reflects an inherited

characteristic of the VRP-SA along the road network upgrade process. At the outset, dispatching AVs in routing tasks provides little or no benefit compared to HDVs. In the end, dispatching AVs is most beneficial but the problem structure is reduced back to a CVRP. Hence, high-quality solutions to the VRP-SA are the most valuable and yet the most difficult to obtain during the intermediate phase of semi-autonomous driving.

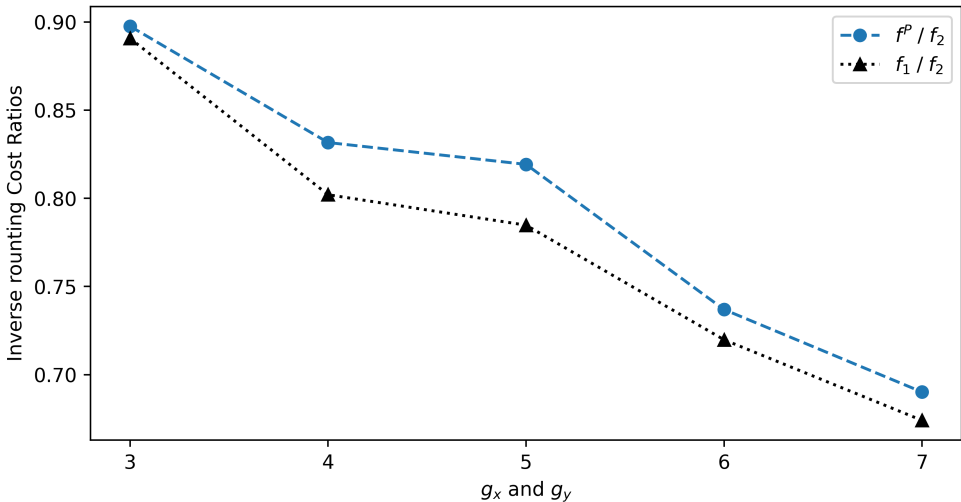


Figure 9: Average inverse routing cost ratios under various densities of AV-enabled roads

8 Conclusion and Future Directions

To conclude this paper, we introduce a novel variant of the vehicle routing problem, termed VRP-SA, designed for the semi-autonomous environment anticipated in the near future. We provide both a rigorous MILP model and an efficient solution approach. Extensive numerical experiments using a benchmark VRP dataset demonstrate the potential and benefits of deploying AV fleets for routing tasks, even with limited infrastructure support.

This paper represents a pioneering effort in exploring the impact of a semi-autonomous environment on a broad class of operations research problems related to fleet management and transportation networks. Although our focus is specifically on vehicle routing, we believe our findings can inspire further research in related areas. For example, a relevant question might be: Which subset of AV-enabled roads should be upgraded first in a city to support AV deployment? This could lead to novel network design problems that are not yet characterized by existing frameworks.

Regarding the VRP-SA itself, there is potential for further improvement in solution quality. The two-phase algorithm currently decomposes customer assignment and sequencing, limiting its scope to local search. Future research could investigate more advanced algorithms that enable a more comprehensive exploration of the solution space. Potential approaches include Lagrangian relaxation and Benders decomposition, which can exploit the special structures of the original

MILP, as well as column generation techniques based on the set partitioning formulation.

References

- [1] Philippe Augerat et al. “Computational results with a branch and cut code for the capacitated vehicle routing problem”. In: (1995).
- [2] Roberto Baldacci and Aristide Mingozzi. “A unified exact method for solving different classes of vehicle routing problems”. In: *Mathematical Programming* 120 (2009), pp. 347–380.
- [3] John E Bell and Patrick R McMullen. “Ant colony optimization techniques for the vehicle routing problem”. In: *Advanced Engineering Informatics* 18.1 (2004), pp. 41–48.
- [4] Colin Beresford. *Honda Legend Sedan with Level 3 Autonomy Available for Lease in Japan*. 2021. URL: <https://www.caranddriver.com/news/a35729591/honda-legend-level-3-autonomy-leases-japan/>.
- [5] Kris Braekers, Katrien Ramaekers, and Inneke Van Nieuwenhuysse. “The vehicle routing problem: State of the art classification and review”. In: *Computers & Industrial Engineering* 99 (2016), pp. 300–313.
- [6] Julien Bramel and David Simchi-Levi. “A location based heuristic for general routing problems”. In: *Operations Research* 43.4 (1995), pp. 649–660.
- [7] Olli Bräysy and Michel Gendreau. “Vehicle routing problem with time windows, Part I: Route construction and local search algorithms”. In: *Transportation science* 39.1 (2005), pp. 104–118.
- [8] Olli Bräysy and Michel Gendreau. “Vehicle routing problem with time windows, Part II: Metaheuristics”. In: *Transportation Science* 39.1 (2005), pp. 119–139.
- [9] Geoff Clarke and John W Wright. “Scheduling of vehicles from a central depot to a number of delivery points”. In: *Operations Research* 12.4 (1964), pp. 568–581.
- [10] George B Dantzig and John H Ramser. “The truck dispatching problem”. In: *Management Science* 6.1 (1959), pp. 80–91.
- [11] Martin Desrochers, Jacques Desrosiers, and Marius Solomon. “A new optimization algorithm for the vehicle routing problem with time windows”. In: *Operations Research* 40.2 (1992), pp. 342–354.
- [12] Sevgi Erdoğan and Elise Miller-Hooks. “A green vehicle routing problem”. In: *Transportation Research Part E: Logistics and Transportation Review* 48.1 (2012), pp. 100–114.
- [13] Matteo Fischetti, Paolo Toth, and Daniele Vigo. “A branch-and-bound algorithm for the capacitated vehicle routing problem on directed graphs”. In: *Operations Research* 42.5 (1994), pp. 846–859.

- [14] Marshall L Fisher and Ramchandran Jaikumar. “A generalized assignment heuristic for vehicle routing”. In: *Networks* 11.2 (1981), pp. 109–124.
- [15] Ricardo Fukasawa et al. “Robust branch-and-cut-and-price for the capacitated vehicle routing problem”. In: *Mathematical programming* 106 (2006), pp. 491–511.
- [16] Ed Garsten. *Einride Gets Go-Ahead For Driverless Electric Trucks On Public Roads*. 2022. URL: <https://www.forbes.com/sites/edgarsten/2022/06/23/einride-gets-go-ahead-for-driverless-trucks-on-public-roads/?sh=1b6be34ac0c7>.
- [17] Billy E Gillett and Leland R Miller. “A heuristic algorithm for the vehicle-dispatch problem”. In: *Operations Research* 22.2 (1974), pp. 340–349.
- [18] Bruce Golden et al. “The fleet size and mix vehicle routing problem”. In: *Computers & Operations Research* 11.1 (1984), pp. 49–66.
- [19] Chana J. Haboucha, Robert Ishaq, and Yoram Shiftan. “User preferences regarding autonomous vehicles”. In: *Transportation Research Part C: Emerging Technologies* 78 (2017), pp. 37–49. ISSN: 0968-090X.
- [20] ANDREW J. HAWKINS. *Waymo’s driverless vehicles are picking up passengers in downtown Phoenix*. 2022. URL: <https://www.theverge.com/2022/8/29/23323593/waymo-driverless-vehicles-passengers-downtown-phoenix>.
- [21] Jörg Homberger and Hermann Gehring. “Two evolutionary metaheuristics for the vehicle routing problem with time windows”. In: *INFOR: Information Systems and Operational Research* 37.3 (1999), pp. 297–318.
- [22] Arif Imran, Said Salhi, and Niaz A. Wassan. “A variable neighborhood-based heuristic for the heterogeneous fleet vehicle routing problem”. In: *European Journal of Operational Research* 197.2 (2009), pp. 509–518.
- [23] Sae International. “Taxonomy and definitions for terms related to driving automation systems for on-road motor vehicles”. In: *SAE international* 4970.724 (2018), pp. 1–5.
- [24] Çağrı Koç et al. “Thirty years of heterogeneous vehicle routing”. In: *European Journal of Operational Research* 249.1 (2016), pp. 1–21.
- [25] Antoon WJ Kolen, AHG Rinnooy Kan, and Harry WJM Trienekens. “Vehicle routing with time windows”. In: *Operations Research* 35.2 (1987), pp. 266–273.
- [26] Wouter Kool, Herke van Hoof, and Max Welling. “Attention, Learn to Solve Routing Problems!” In: *International Conference on Learning Representations*. 2019.
- [27] Jan Karel Lenstra and AHG Rinnooy Kan. “Complexity of vehicle routing and scheduling problems”. In: *Networks* 11.2 (1981), pp. 221–227.
- [28] Alex Leslie and Dan Murray. *An Analysis of the Operational Costs of Trucking*. Tech. rep. American Transportation Research Institute, 2022.

- [29] Sirui Li, Zhongxia Yan, and Cathy Wu. “Learning to delegate for large-scale vehicle routing”. In: *Advances in Neural Information Processing Systems*. Ed. by A. Beygelzimer et al. 2021.
- [30] Xiangyong Li, Peng Tian, and Y.P. Aneja. “An adaptive memory programming metaheuristic for the heterogeneous fixed fleet vehicle routing problem”. In: *Transportation Research Part E: Logistics and Transportation Review* 46.6 (2010), pp. 1111–1127.
- [31] Canhong Lin et al. “Survey of green vehicle routing problem: past and future trends”. In: *Expert Systems with Applications* 41.4 (2014), pp. 1118–1138.
- [32] Clair E Miller, Albert W Tucker, and Richard A Zemlin. “Integer programming formulation of traveling salesman problems”. In: *Journal of the ACM (JACM)* 7.4 (1960), pp. 326–329.
- [33] Jose C. Molina et al. “The heterogeneous vehicle routing problem with time windows and a limited number of resources”. In: *Engineering Applications of Artificial Intelligence* 94 (2020), p. 103745.
- [34] Jairo R Montoya-Torres et al. “A literature review on the vehicle routing problem with multiple depots”. In: *Computers & Industrial Engineering* 79 (2015), pp. 115–129.
- [35] Mohammadreza Nazari et al. “Reinforcement learning for solving the vehicle routing problem”. In: *Advances in Neural Information Processing Systems* 31 (2018).
- [36] David Pisinger and Stefan Ropke. “A general heuristic for vehicle routing problems”. In: *Computers & Operations Research* 34.8 (2007), pp. 2403–2435.
- [37] Christian Prins. “Two memetic algorithms for heterogeneous fleet vehicle routing problems”. In: *Engineering Applications of Artificial Intelligence* 22.6 (2009). *Artificial Intelligence Techniques for Supply Chain Management*, pp. 916–928.
- [38] Jacques Renaud, Gilbert Laporte, and Faye F Boctor. “A tabu search heuristic for the multi-depot vehicle routing problem”. In: *Computers & Operations Research* 23.3 (1996), pp. 229–235.
- [39] Jessica Rodríguez-Pereira et al. “The Steiner Traveling Salesman Problem and its extensions”. In: *European Journal of Operational Research* 278.2 (2019), pp. 615–628.
- [40] Martin WP Savelsbergh and Marc Sol. “The general pickup and delivery problem”. In: *Transportation Science* 29.1 (1995), pp. 17–29.
- [41] Michael Schneider, Andreas Stenger, and Dominik Goeke. “The electric vehicle-routing problem with time windows and recharging stations”. In: *Transportation Science* 48.4 (2014), pp. 500–520.
- [42] Marius M Solomon. “Algorithms for the vehicle routing and scheduling problems with time window constraints”. In: *Operations Research* 35.2 (1987), pp. 254–265.
- [43] Paolo Toth and Daniele Vigo. *Vehicle routing: problems, methods, and applications*. SIAM, 2014.

- [44] Eduardo Uchoa et al. “New benchmark instances for the capacitated vehicle routing problem”. In: *European Journal of Operational Research* 257.3 (2017), pp. 845–858.
- [45] Thibaut Vidal. “Hybrid genetic search for the CVRP: Open-source implementation and SWAP* neighborhood”. In: *Computers & Operations Research* 140 (2022), p. 105643. ISSN: 0305-0548.
- [46] Thibaut Vidal et al. “A unified solution framework for multi-attribute vehicle routing problems”. In: *European Journal of Operational Research* 234.3 (2014), pp. 658–673.

A Proofs of Lemma 4.1, Lemma 4.2, and Proposition 4.3

Lemma 4.1. *In an optimal solution to the STSP in a directed graph, a node can be visited at most n times, where n is the number of required nodes in the graph.*

Proof. Suppose that there exists an optimal route P^* for a given STSP instance. Denote by u and v two consecutive required nodes in P^* and by $P(u, v) \subseteq P^*$ the sub-path between u and v . Then, every node $x \in P(u, v)$ is visited only once in the scope of $P(u, v)$ as $P(u, v)$ is the minimum-cost path between u and v and there is no positive cycle in any minimum-cost paths. Then, if x is not the depot, the number of times x can be visited in the optimal route P^* is upper bounded by $n - 1$ as it can potentially appear in the sub-paths between any pairs of consecutive required nodes. If x happens to be the depot, this upper bound is n . Furthermore, the example depicted in Figure 10a demonstrates that the upper bound is tight. In a star network, all six nodes are required nodes with node 0 specified as the depot. Any sequences visiting nodes 1 to 5 exactly once are optimal. In all the optimal solutions to the STSP, node 0 is visited 6 times. The pattern can be found in a more general network where all required nodes are located in different isolated regions that can only be accessed via a single gateway. \square

Lemma 4.2. *In an optimal solution to the STSP in a directed graph, an edge can be traversed at most $n - 1$ times, where n is the number of required nodes in the graph.*

Proof. The formal proof of Lemma 4.2 is similar to that of Lemma 4.1 except that the tight upper bound is demonstrated by another example depicted in Figure 10b. In a one-way-dominated network shown in Figure 10b, nodes 0, 6, 8, and 10 are required nodes with node 0 specified as the depot. An optimal solution to the STSP is $(0, 1, 2, 6, 5, 1, 2, 3, 8, 7, 5, 1, 2, 3, 4, 10, 9, 7, 5, 1, 0)$. Node 1 is visited 4 times and edge $(1, 2)$ is traversed 3 times. The pattern can be found in a more general network where all required nodes are located in different isolated one-way-dominated regions that can only be accessed via an inevitable passage. \square

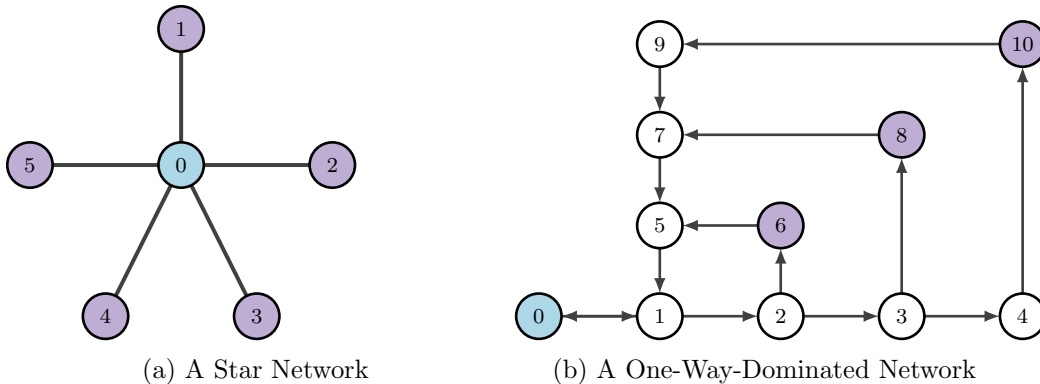


Figure 10: Two types of networks to prove tight upper bounds in Lemma 4.1 and Lemma 4.2

Proposition 4.3. *Let $P(m)$ be the route of vehicle m in the optimal solution to the VRP-SA. Let W be the capacity of vehicle m . Let $\{d_i : i = 1, \dots, |D|\}$ be a non-decreasing sequence indicating the demands of customer set D . Then, a node $v \in P(m)$ can be visited by vehicle m at most $k + 1$ times, and an edge (u, v) , $\forall u, v \in P(m)$ can be traversed by vehicle m at most k times, where k is defined as the largest integer $j = 1, \dots, |D|$ satisfying $\sum_{i=1}^j d_i \leq W$.*

Proof. Suppose $D(m)$ is the set of customers served by vehicle m in the optimal solution and o is the depot. Then, $P(m)$ is the optimal solution to the STSP in the same graph with $D(m) \cup \{o\}$ as the set of required nodes. Based on Lemma 4.2, the upper bound of the number of times v being visited and (u, v) being visited are $|D(m)| + 1$ and $|D(m)|$ respectively. By definition, k is the maximum number of customers vehicle m can potentially serve under any circumstances, meaning that $|D(m)| \leq k$. Thus, the proposition holds. \square

B Flexible Travel Time for Autonomous Vehicles

In this section, we further assume an AV is allowed to increase or decrease its speed to some extent when it is cruising along a road segment (i, j) . Then, an AV can flexibly adjust the travel time on (i, j) as long as the adjustment is within a threshold, which further enlarges the temporal feasible space of the problem. Define $\underline{\gamma}_{ij}$ ($\bar{\gamma}_{ij}$) as the *minimum (maximum) adjustment factor* for the travel time on road segment (i, j) . Then, $[\underline{\gamma}_{ij}\Delta t_{ij}, \bar{\gamma}_{ij}\Delta t_{ij}]$ is the corresponding flexible travel time interval. In this setting, Constraint 11 in the MILP in Section 4 is removed and Constraint 10 is generalized to Constraints 33 and 34 for every AV $m \in M^a$. Note that the constraints corresponding to HDVs are kept intact.

$$t_{jm} \geq t_{im} + \underline{\gamma}_{ij}\Delta t_{ijm} + T(x_{ijm} - 1), \quad \forall (i, j) \in E_e, m \in M^a, \quad (33)$$

$$t_{jm} \leq t_{im} + \bar{\gamma}_{ij}\Delta t_{ijm} + T(1 - x_{ijm}), \quad \forall (i, j) \in E_e, m \in M^a. \quad (34)$$

One may argue that the flexible travel time assumption for the AV fleet is ill-conceived for two reasons: (1) It can impair network efficiency by blocking the traffic in some primary avenues. (2) It can affect the routing cost and change the objective of the problem. For this, we emphasize that it only generalizes the model and provides the possibility to design a better dispatching and routing strategy in the semi-autonomous environment. The adjustment factor of every road segment can be determined separately and designed according to the input network. Also, we admit a linear mapping between the routing cost and the travel time, which makes the problem objective easily adaptable to cases with flexible travel time.

B.1 Effects on the Re-Scheduling MILP

Following the notations used in Section 6.1, when the flexible travel time assumption is adopted, the time interval of any sub-route r can be independently adjusted by a factor of $\underline{\gamma}_r$ for shrinking

or $\bar{\gamma}_r$ for expanding, where $\underline{\gamma}_r$ and $\bar{\gamma}_r$ are determined in Equations 35 and 36:

$$\underline{\gamma}_r = \frac{1}{\Delta t_r} \sum_{(i,j) \in r} \underline{\gamma}_{ij} \Delta t_{ij} \quad (35)$$

$$\bar{\gamma}_r = \frac{1}{\Delta t_r} \sum_{(i,j) \in r} \bar{\gamma}_{ij} \Delta t_{ij} \quad (36)$$

Figure 11 illustrates how this assumption results in a larger feasible space of the re-scheduling FRP. The original schedules are the same as the ones described in Figure 5, except that the second ordinary sub-route of vehicle m_1 is longer. Consequently, the AV-enabled sub-route between the second and the third ordinary sub-routes becomes shorter. In this case, the re-scheduling FRP with fixed travel times is infeasible, as shifting the entire routing schedule of vehicle m_2 cannot bypass all overlaps. However, under the flexible travel time assumption, we can further delay the second ordinary sub-route of vehicle m_2 by an extra δ' to eliminate the overlap. This adjustment is equivalent to increasing the travel time of the preceding AV-enabled sub-route by δ' .

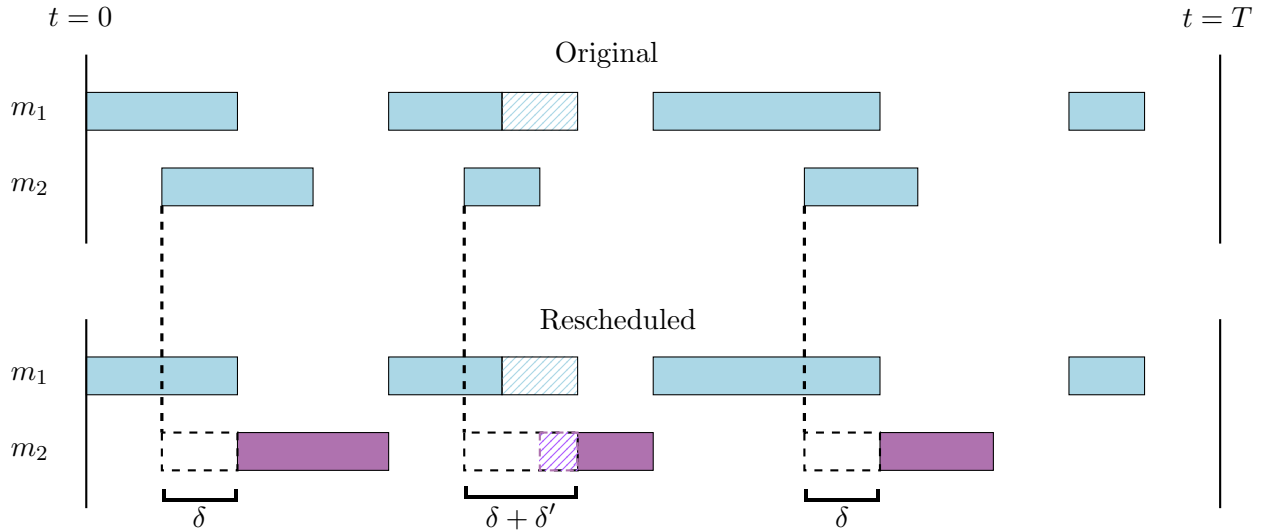


Figure 11: The illustration of the re-scheduling FRP with flexible travel time

To facilitate this more powerful re-scheduling strategy, we can simply relax the hard constraints of fixed travel time accumulation in 24 to 25 to the soft constraints shown in 37 to 40.

$$t_r^1 \leq \bar{t}_m + \sum_{r': r' \prec r} \bar{\gamma}_{r'} \Delta t_{r'}, \quad r \in R, \quad (37)$$

$$t_r^1 \geq \bar{t}_m + \sum_{r': r' \prec r} \underline{\gamma}_{r'} \Delta t_{r'}, \quad r \in R, \quad (38)$$

$$t_r^2 \leq t_r^1 + \bar{\gamma}_r \Delta t_r, \quad \forall r \in R, \quad (39)$$

$$t_r^2 \geq t_r^1 + \underline{\gamma}_r \Delta t_r, \quad \forall r \in R. \quad (40)$$

C The Re-Routing MILP

The re-routing MILP takes as input an expanded graph G_e , a set of customers D , an end time of operation T , and a set of *infeasible time intervals* Q , where each interval has a start times a_q and an end time b_q . During each infeasible time interval, the budget of remote controllers is already exhausted by other AVs. The objective is to find a minimum-cost tour visiting all customers exactly once.

We adopt most notations from Section 4 and overwrite the following for simplicity: Define a binary decision variable x_{ij} for every edge $(i, j) \in E_e$ to indicate whether the edge is selected in the route. Define a binary decision variable y_i for every customer $i \in D_e$ to indicate whether a duplicate of the customer in the expanded graph is served. Define a continuous variable $t_i \in [0, T]$ for every node $i \in V_e$ to represent the timestamp of the AV visiting the node. Define a binary decision variable α_{qij} for every $q \in Q$ and every edge $(i, j) \in E_e$, with $\alpha_{qij} = 1$ indicating the timestamp of the vehicle exiting edge (i, j) is later than the start time of interval q . Define a binary decision variable β_{qij} for every $q \in Q$ and every edge $(i, j) \in E_e$, with $\beta_{qij} = 1$ indicating the timestamp of the vehicle entering edge (i, j) is earlier than the end time of interval q . Then, the re-routing MILP can be formulated as follows.

$$\begin{aligned}
& \min_{\mathbf{x}, \mathbf{y}, \mathbf{t}, \boldsymbol{\alpha}, \boldsymbol{\beta}} && \sum_{(i,j) \in E_e^a} c_{ij}^1 x_{ij} + \sum_{(i,j) \in E_e^o} c_{ij}^2 x_{ij} \\
& \text{s.t.} && \sum_{j \in \delta^-(i)} x_{ij} = \sum_{j \in \delta^+(i)} x_{ji}, \quad \forall i \in V_e - \{o, s\}, \\
& && \sum_{j \in \delta^-(o)} x_{oj} = \sum_{j \in \delta^+(s)} x_{js} \leq 1, \\
& && \sum_{i \in DV(j)} y_i = 1, \quad \forall j \in D, \\
& && \sum_{j \in \delta^+(i)} x_{ji} \geq y_i, \quad \forall i \in D_e, \\
& && x_{ij} \leq y_i, \quad \forall (i, j) \in A, \\
& && t_j \geq t_i + \Delta t_{ij} + T(x_{ij} - 1), \quad \forall (i, j) \in E_e, \\
& && t_s = t_o + \sum_{(i,j) \in E_e} \Delta t_{ij} x_{ij} \leq T, \\
& && t_j \leq a_q + T\alpha_{qij}, \quad \forall q \in Q, \forall (i, j) \in E_e^o, \\
& && t_j \geq a_q + T(\alpha_{qij} - 1), \quad \forall q \in Q, \forall (i, j) \in E_e^o, \\
& && b_q \leq t_i + T\beta_{qij}, \quad \forall q \in Q, \forall (i, j) \in E_e^o, \\
& && b_q \geq t_i + T(\beta_{qij} - 1), \quad \forall q \in Q, \forall (i, j) \in E_e^o, \\
& && \alpha_{qij} + \beta_{qij} + x_{ij} \leq 2, \quad \forall q \in Q, \forall (i, j) \in E_e^o
\end{aligned}$$

D Experimental Results

The rounded routing costs for the VRP-SA instances, which correspond to Figure 7, are listed in Table 3 below.

Table 3: Routing cost for the VRP-SA instances

Instances	Cost by HDVs	Cost by HDVs + AVs	
		w.o. re-routing priority	w. re-routing priority
P-n16-k8	600	387	386
P-n19-k2	280	251	247
P-n20-k2	282	249	249
P-n21-k2	282	258	258
P-n22-k2	288	269	243
P-n22-k8	750	508	472
P-n23-k8	694	474	475
P-n40-k5	590	501	455
P-n45-k5	650	563	532
P-n50-k7	700	645	579
P-n50-k8	798	627	624
P-n50-k10	880	682	680
P-n51-k10	958	779	755
P-n55-k7	710	615	601
P-n55-k10	870	685	689
P-n55-k15	1204	895	880
P-n60-k10	926	876	856
P-n60-k15	1230	971	963
P-n65-k10	992	928	913
P-n70-k10	1034	988	926
P-n76-k4	742	759	722
P-n76-k5	780	772	766
P-n101-k4	876	857	878